NASA/CR-2006-214515

Optimization of Blended Wing Body Composite Panels Using Both NASTRAN and Genetic Algorithm

Andrew E. Lovejoy
Analytical Services & Materials, Inc., Hampton, Virginia

October 2006

The NASA STI Program Office . . . in Profile

Since its founding, NASA has been dedicated to the advancement of aeronautics and space science. The NASA Scientific and Technical Information (STI) Program Office plays a key part in helping NASA maintain this important role.

The NASA STI Program Office is operated by Langley Research Center, the lead center for NASA's scientific and technical information. The NASA STI Program Office provides access to the NASA STI Database, the largest collection of aeronautical and space science STI in the world. The Program Office is also NASA's institutional mechanism for disseminating the results of its research and development activities. These results are published by NASA in the NASA STI Report Series, which includes the following report types:

- TECHNICAL PUBLICATION. Reports of completed research or a major significant phase of research that present the results of NASA programs and include extensive data or theoretical analysis. Includes compilations of significant scientific and technical data and information deemed to be of continuing reference value. NASA counterpart of peer-reviewed formal professional papers, but having less stringent limitations on manuscript length and extent of graphic presentations.

- TECHNICAL MEMORANDUM. Scientific and technical findings that are preliminary or of specialized interest, e.g., quick release reports, working papers, and bibliographies that contain minimal annotation. Does not contain extensive analysis.

- CONTRACTOR REPORT. Scientific and technical findings by NASA-sponsored contractors and grantees.

- CONFERENCE PUBLICATION. Collected papers from scientific and technical conferences, symposia, seminars, or other meetings sponsored or co-sponsored by NASA.

- SPECIAL PUBLICATION. Scientific, technical, or historical information from NASA programs, projects, and missions, often concerned with subjects having substantial public interest.

- TECHNICAL TRANSLATION. English-language translations of foreign scientific and technical material pertinent to NASA's mission.

Specialized services that complement the STI Program Office's diverse offerings include creating custom thesauri, building customized databases, organizing and publishing research results ... even providing videos.

For more information about the NASA STI Program Office, see the following:

- Access the NASA STI Program Home Page at ***http://www.sti.nasa.gov***

- E-mail your question via the Internet to help@sti.nasa.gov

- Fax your question to the NASA STI Help Desk at (301) 621-0134

- Phone the NASA STI Help Desk at (301) 621-0390

- Write to:
  NASA STI Help Desk
  NASA Center for AeroSpace Information
  7121 Standard Drive
  Hanover, MD 21076-1320

NASA/CR-2006-214515

Optimization of Blended Wing Body Composite Panels Using Both NASTRAN and Genetic Algorithm

Andrew E. Lovejoy
Analytical Services & Materials, Inc., Hampton, Virginia

National Aeronautics and
Space Administration

Langley Research Center
Hampton, Virginia 23681-2199

Prepared for Langley Research Center
under Contract NNNL04AA06Z

October 2006

Available from:

NASA Center for AeroSpace Information (CASI)
7121 Standard Drive
Hanover, MD 21076-1320
(301) 621-0390

National Technical Information Service (NTIS)
5285 Port Royal Road
Springfield, VA 22161-2171
(703) 605-6000

Table of Contents

List of Figures

List of Tables

Abstract

The blended wing body (BWB) is a concept that has been investigated for improving the performance of transport aircraft. A trade study was conducted by evaluating four regions from a BWB design characterized by three fuselage bays and a 400,000 lb. gross take-off weight (GTW). This report describes the structural optimization of these regions via computational analysis and compares them to the baseline designs of the same construction. The identified regions were simplified for use in the optimization. The regions were represented by flat panels having appropriate classical boundary conditions and uniform force resultants along the panel edges. Panel edge tractions and internal pressure values applied during the study were those determined by nonlinear NASTRAN analyses. Only one load case was considered in the optimization analysis for each panel region. Optimization was accomplished using both NASTRAN solution 200 and Genetic Algorithm (GA), with constraints imposed on stress, buckling and minimum thicknesses. The NASTRAN optimization analyses often resulted in infeasible solutions due to violation of the constraints, whereas the GA enforced satisfaction of the constraints and therefore always ensured a feasible solution. However, both optimization methods encountered difficulties when the number of design variables was increased. In general, the optimized panels weighed less than the comparable baseline panels.

Introduction

Over the past decade, there has been great interest in improving the performance of transport aircraft. One concept that has been investigated, initially by McDonnell Douglas, and subsequently by Boeing who acquired McDonnell Douglas, is the Blended Wing Body (BWB) as shown in Figure 1. The BWB concept is a hybrid that combines features of the flying wing with features of conventional transport aircraft. Such a configuration has the advantage of simultaneously increasing both fuel efficiency and payload [1, 2]. Early in the formulation of the BWB concept, it was realized that requiring conventional structural configurations limited the potential design space. Therefore, the conventional pressurized cabin structure was abandoned with the expectation that future structural concepts would be developed that were capable of sustaining the encountered BWB loads [2]. As a result, initial BWB research focused on the aerodynamic, stability and control issues (flying characteristics), and included wind tunnel tests at NASA Langley Research Center (LaRC). Figures 2 and 3 show BWB wind tunnel test models in the 14x22 foot and the National Transonic Facility (NTF), respectively. While later studies have continued to address BWB flying characteristics, including noise and propulsion issues, recent years have seen an increased focus on the structural performance of the BWB [3-7], because structures technology does not yet satisfy the expected capabilities.

Throughout the development of BWB designs, many sizes and configurations have been studied. A recent BWB configuration is a 3-bay (three internal bays), approximately 400,000 lb. GTW, twin-engine design that makes substantial use of advanced/composite materials (see Figure 4). The structural configuration subjects the majority of the BWB panels to combined loads, and panels within the pressurized cabin (shaded region in Figure 4) are, additionally, subjected to internal pressure. Therefore, the design and sizing of these panels requires more thorough examination and analysis than conventional transport aircraft components that have traditional and less complex load paths. Several sizing and optimization studies have been conducted on BWB-like structures [3, 5, 6]. The current work focuses on the optimization of representative BWB-type skin panels of either stitched-composite or integrally-stitched sandwich construction that are defined in the following section.

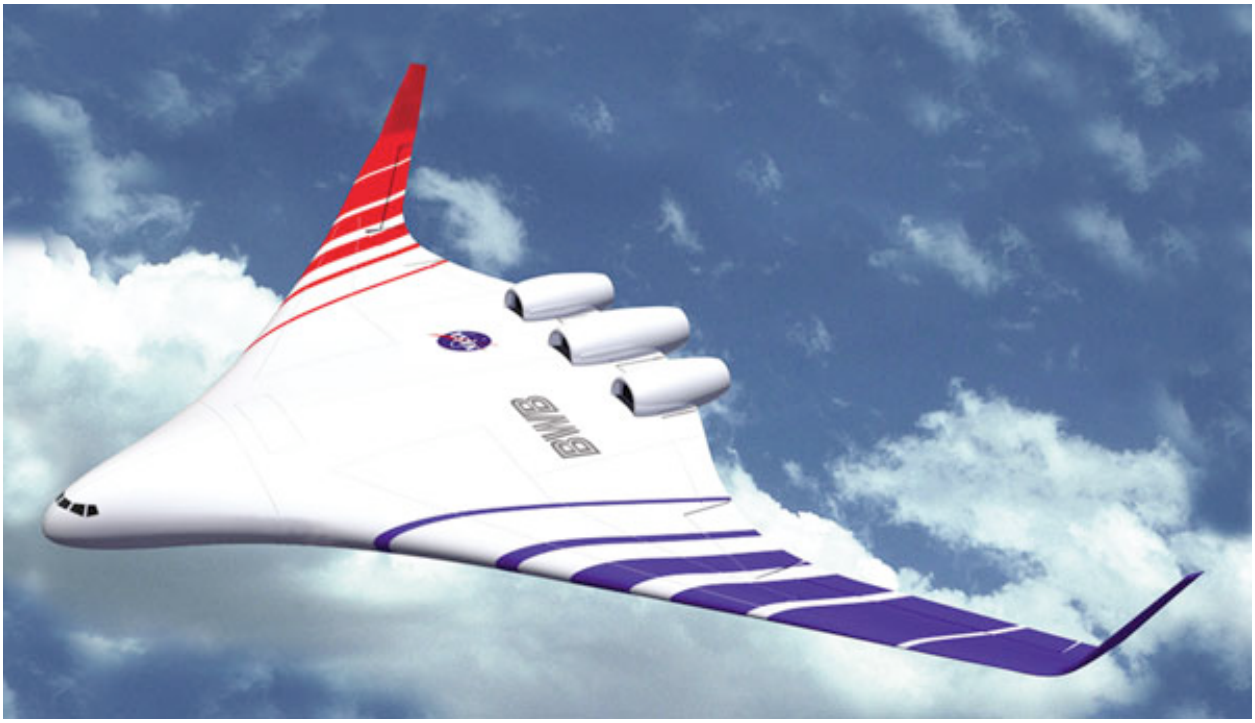

Figure 1: BWB design concept

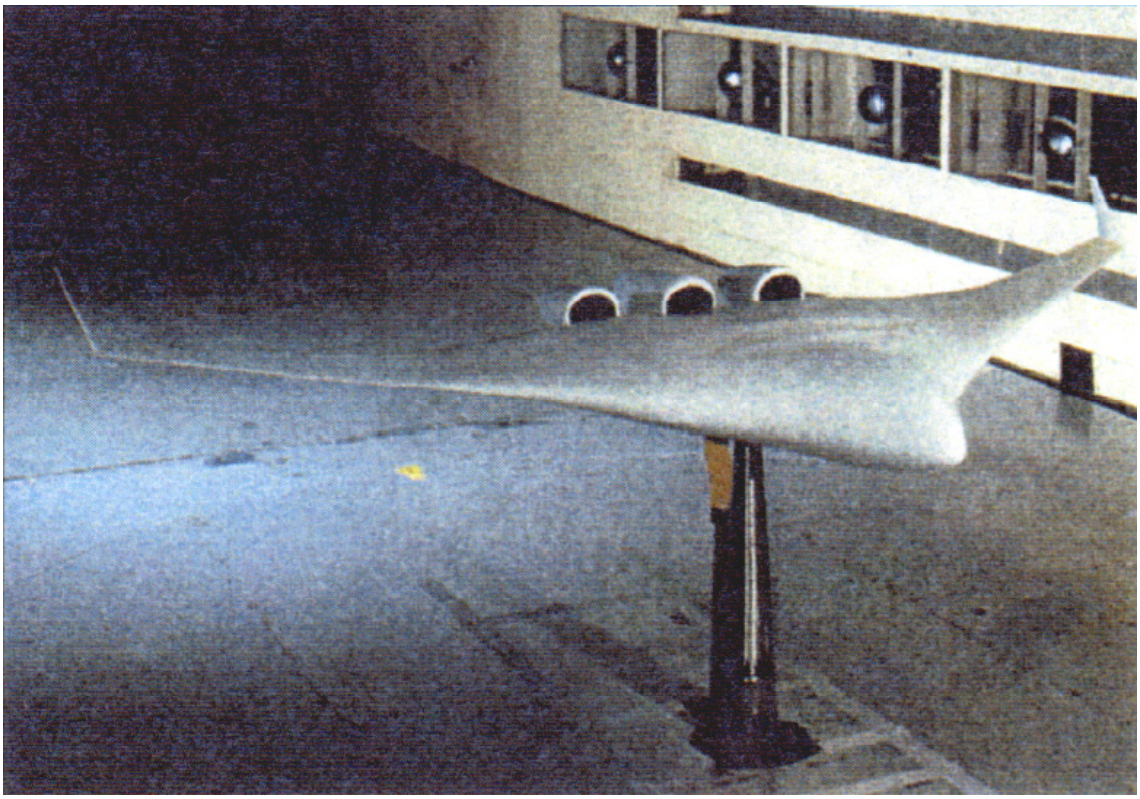

Figure 2: BWB design concept tested in LaRC's 14x22 foot wind tunnel

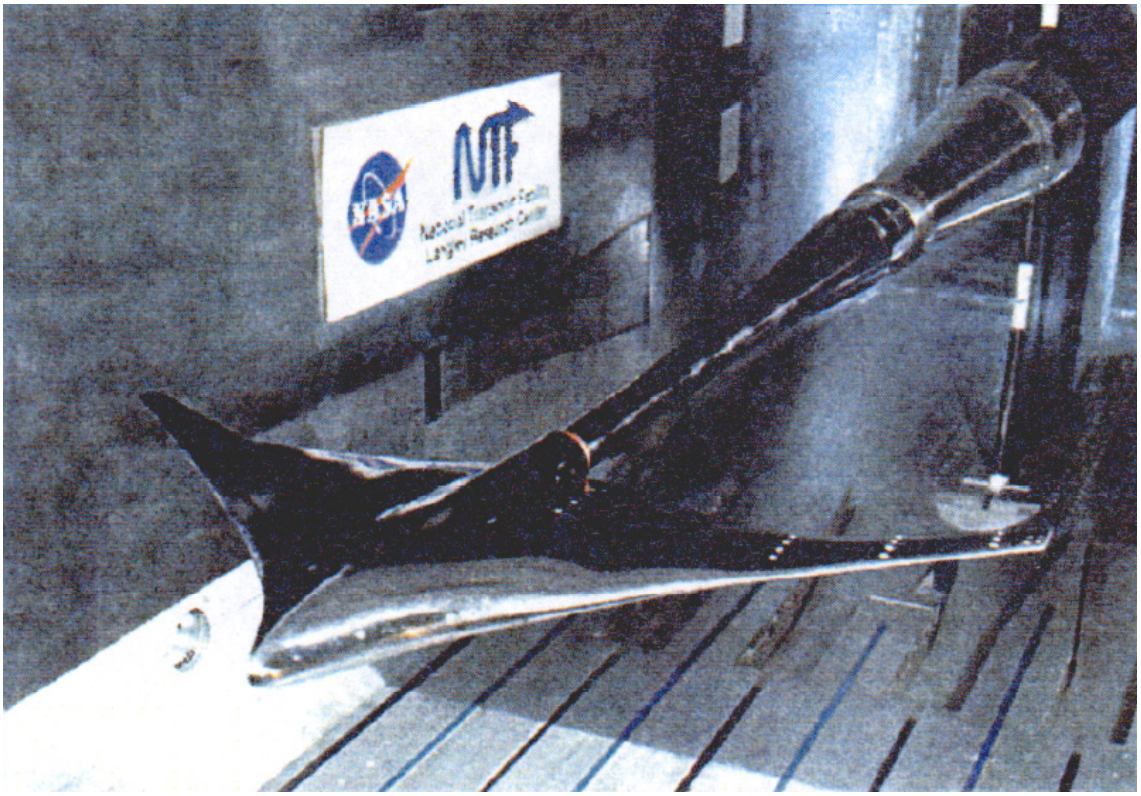

Figure 3: BWB design concept tested in LaRC's NTF

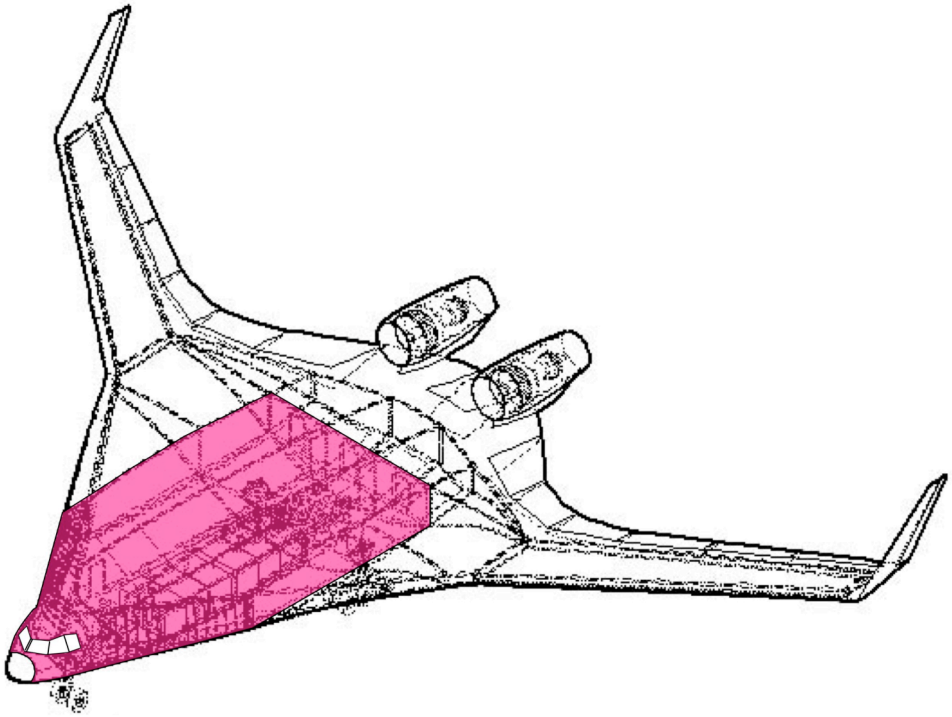

Figure 4: 3-bay, twin-engine BWB design configuration

Requirements / Panel Selection

The 3-bay BWB configuration shown in Figure 4 was subjected to numerous load cases for design and sizing. A NASTRAN finite element model, shown in Figure 5, was obtained from Boeing and used to develop an understanding of the BWB design, structure and loading. In order to accurately study buckling and nonlinear response, the BWB NASTRAN model was modified using several existing and new author-written PATRAN Command Language (PCL) programs. Requirements for the PCL programs were developed, the code was written, and the programs verified using simple examples. These PCL programs perform many modifications, including but not limited to, changing bar elements to beam elements, removing offsets in laminates and removing offsets for shell properties. Removal of laminate and shell offsets required the creation of a dummy material that was used to create a new laminate that includes a ply of the dummy material. The thickness of the dummy ply is chosen so that the no offset is required, and can thus be removed from the original property definition. Laminate and shell modifications did not change the structural response compared to the model having laminate and shell offsets included. Remove of beam offsets was also required. Unfortunately, the beam property definition depends, in part, upon the beam element axis, the orientation vector and the shear center offset vector. Normally, many beam elements may have the same property definition. However, removal of the offset vector for beams within the same property can require creation of a new property for each beam element to properly remove the offsets. To avoid the difficult task of creating a new property set for each beam, it was decided remove the offset, but not to calculate new beam section properties that account for the offset. This approximation resulted in structural response that was within about 1% of the previous results, so it was determined acceptable to simply remove the beam offsets and not adjust the section properties.

All PCL programs were implemented on the BWB model through a PATRAN session file. The new nonlinear capable model was utilized to choose the locations to be included in the trade study, and also to determine which load cases are most critical to the trade study locations chosen. Figure 6 shows the finite element meshes used for the upper and lower BWB covers, respectively.

Ten load cases were supplied by Boeing, three of which had variants in which cabin pressure was included. Table 1 defines the load cases utilized in this study, with the "P" designation indicating that the loading is the same as that for the plain numbered load case, but with internal pressure of 9.2 psi included (i.e, "P" = 9.2 psi). NASTRAN solutions 101 (load cases 1-4) and 144 (load cases 5-10P) were conducted to determine nodal loads to be applied during the nonlinear analyses. Figures 7 to 19 show the linear analysis force resultants in the upper and lower covers for the load cases defined in the table. Figures 20 and 21 show the upper and lower cover displacement differential for load cases 9 and 9P, respectively, from linear analyses using nodal loads applied to the nonlinear capable model.

Based upon the force resultants and the deformations, four regions were chosen for the trade study. Regions were chosen so that the panel is bounded by major structural elements, such as ribs, spars and bulkheads. The chosen regions were required to have combined loads, and at least one region was required to have include internal pressure. The four regions are identified in Figure 22, summarized in Table 2 and depicted in Figure 23. Regions 1 and 2 are located in the inner wing area and are subjected to large combined loads. Regions 3 and 4 are in the fuselage section and are subjected to smaller combined loads but than regions 1 and 2, but they include internal pressure.

The panel regions chosen for the BWB trade study have very large radii of curvature. For the trade study, however, they are considered flat to simplify modeling and to avoid potential limitations of the analytical tools that might be used. Also for the purpose of the trade study, regions 1 and 2 are considered to be simply-supported on all edges, and regions 3 and 4 are considered to be clamped on all edges. Lastly, the trade study was further simplified by using uniform force resultants along the edges instead of calculating and applying non-uniform resultants. The value chosen for each force resultant component along an edge was either the dominant value, if there was one, or was the maximum value when no dominant value could be identified. Table 3 shows the edge loads and pressure values for the most critical load cases for the four trade study regions. The edge load and pressure values applied in the study were

those from the nonlinear analysis. The load cases chosen and used for the optimization of each panel are identified in the table by the yellow shading. Sign conventions for the loads are shown in Figure 24.

As indicated in Table 2, regions 1 and 2 are of stitched composite construction. Skins and stringers are built up using stacks that are stitched together and resin infused. Each stack consists of 7 plies and has a stacking sequence of [45/-45/0/90/0/-45/45]. The thicknesses of the plies are 0° = 0.0124 in., 90° = 0.066 in., 45° and -45° = 0.0059 in., resulting in a 0.055 in. total stack thickness. The resulting stack stiffnesses and unnotched strengths for the material used in the current study are shown in Tables 4 and 5, respectively. Regions 3 and 4 are integrally-stitched sandwich skins with composite sandwich frames. The stacks used to construct the sandwich skins and frames are the same as those used in regions 1 and 2.

Figure 25 shows the basic cross-section for each of the panel regions. Stringers and frames are oriented in the aircraft span-wise direction (global x-direction). The local cross-section for the region 1 and 2 panels is shown in Figure 26. Dimensions of the skin and stringer are indicated in the figure. Figure 27 shows the local cross-section for the panels of regions 3 and 4, with dimensions of the sandwich skin and frames indicated. Non-numerical dimensions as indicated in Figures 26 and 27 are used as design variables in the optimization study.

Table 1: Load case definitions

Load Case #	Designation
1	2G Taxi Bump
2	2P Overpressure
3	4.5 Lateral Crash
4	9G FWD Crash
5	-1.0G Push-Over, VC
5P	-1.0G Push-Over, VC, 1P
6	1G, Dynamic Overswing
7	Initial Roll, Vertical Load 0G
8	Initial Roll, Vertical Load 1.67G
9	2.5G, MXTOWT
9P	2.5G, MXTOWT, 1P
10	-1.0G Push-Over, VPTA
10P	-1.0G Push-Over, VPTA, 1P

Table 2: Trade study region descriptions

Region #	Description	Size (in.)
1	Upper cover, inner wing, stitched composite, non-pressurized	34.5 by 94
2	Lower cover, inner wing, stitched composite, non-pressurized	34.5 by 96
3	Upper cover, fuselage, integrally-stitched sandwich composite, pressurized	155 by 96
4	Lower cover, fuselage, integrally-stitched sandwich composite, pressurized	137 by 120

Table 3: Trade study region panel edge loads

Region #	Load Case	Internal Pressure (psi)	Nx (lbs./in.)	Nxy (lbs./in.)	Ny (lbs./in.)	Mx (lbs.-in./in.)	Mxy (lbs.-in./in.)	My (lbs.-in./in.)
1	9	0	-21000 (-20000)	-5500 (-4000)	-2000 (-2000)	15000 (14000)	1000 (900)	500 (450)
	9P	0	-21000 (-20000)	-5500 (-4000)	-2000 (-2000)	15000 (14000)	1000 (900)	500 (450)
	2	0	NA	NA	NA	NA	NA	NA
2	9	0	18000 (15000)	-5500 (-4000)	3000 (2000)	-14000 (-12000)	2000 (1500)	-1500 (-650)
	9P	0	18000 (15000)	-5500 (-4000)	3000 (2000)	-14000 (-12000)	2000 (1500)	-1500 (-650)
	2	0	NA	NA	NA	NA	NA	NA
3	9	0	-2400 (-2000)	-1000 (-700)	-1000 (-1000)	800 (700)	350 (250)	250 (200)
	9P	9.2	-2300 (-2000)	-1200 (-1000)	-1400 (-1300)	700 (500)	400 (400)	-400 (-400)
	2	18.4	-350 (-100)	-150 (-200)	1500 (1800)	200 (50)	150 (150)	-850 (-850)
4	9	0	100 (125)	-150 (-180)	130 (140)	-40 (-45)	60 (55)	-100 (-100)
	9P	9.2	1800 (1700)	-600 (-500)	650 (650)	-550 (-500)	180 (140)	-300 (-300)
	2	18.4	2000 (2100)	-700 (-500)	850 (800)	-700 (-600)	200 (150)	-300 (-250)

Table 4: Stack stiffness properties

	E_x (Msi)	E_y (Msi)	G_{xy} (Msi)	ν_{12}
Tension	10.25	5.07	2.48	0.403
Compression	9.23	4.66	2.26	0.397

Table 5: Stack B-allowable unnotched stress strengths (ksi)

X_T	X_C	Y_T	Y_C	S
105.1	79.2	46.5	37.9	29.9

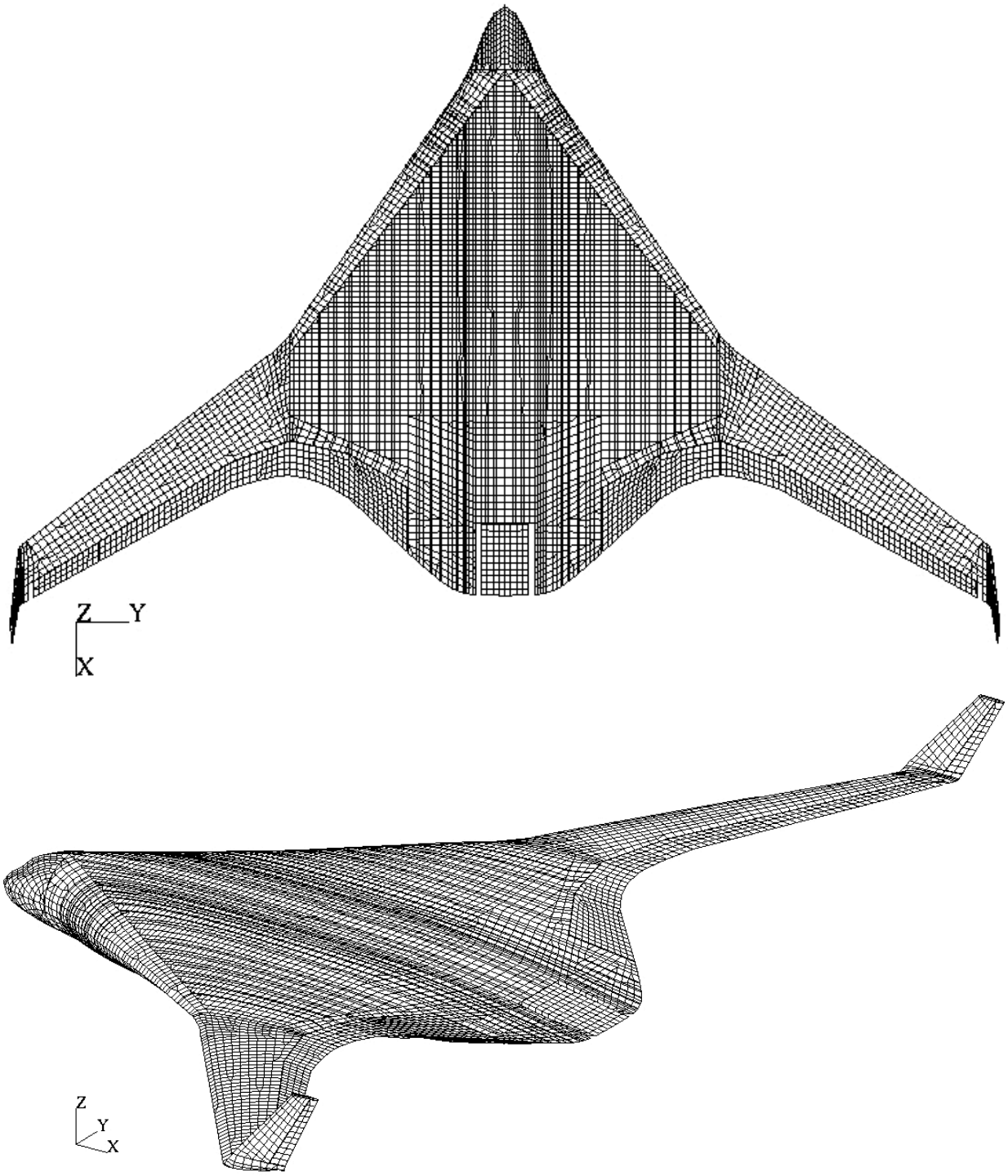

Figure 5: BWB global finite element mesh

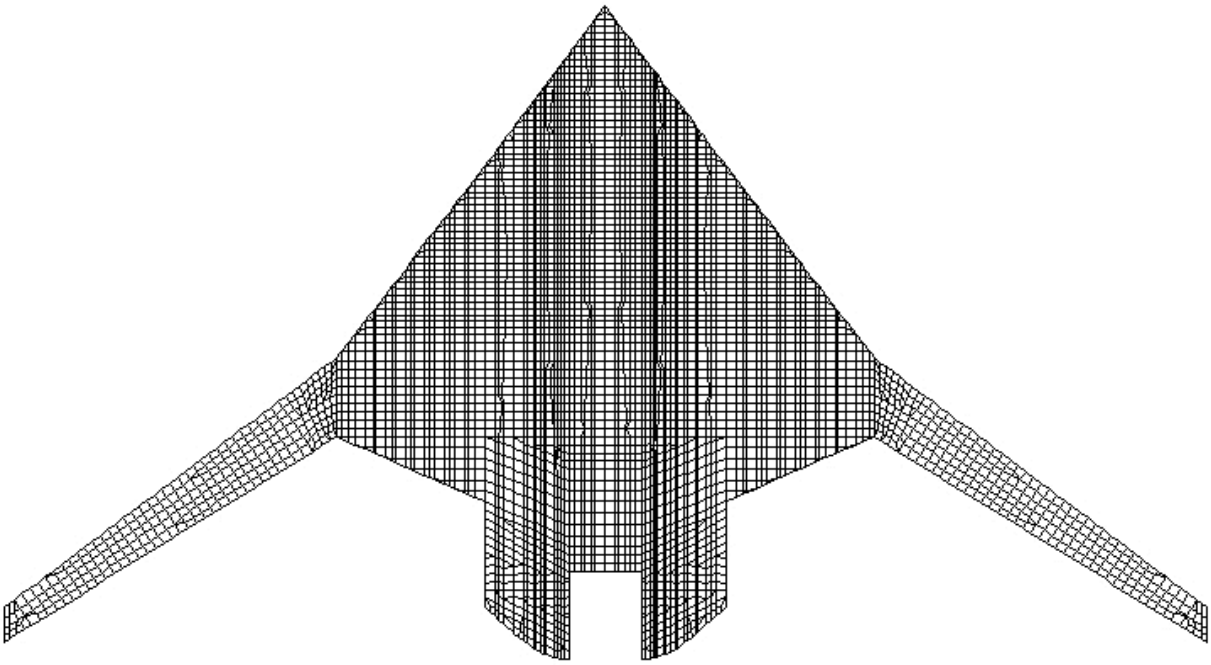

a) upper cover

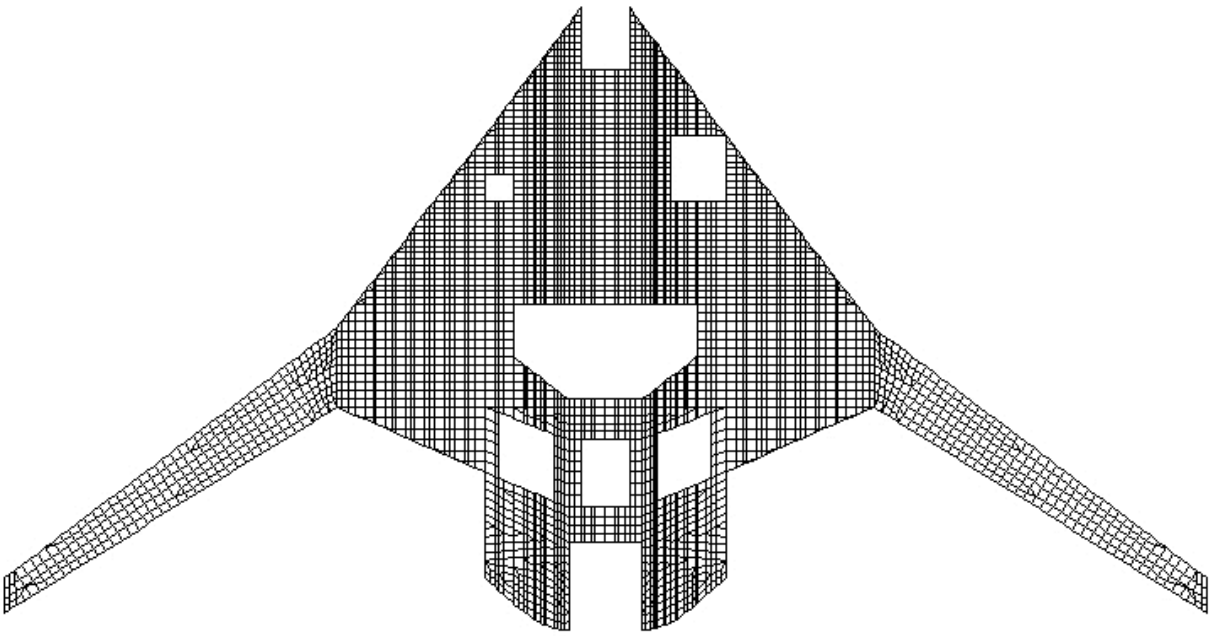

b) lower cover

Figure 6: BWB upper and lower cover finite element meshes

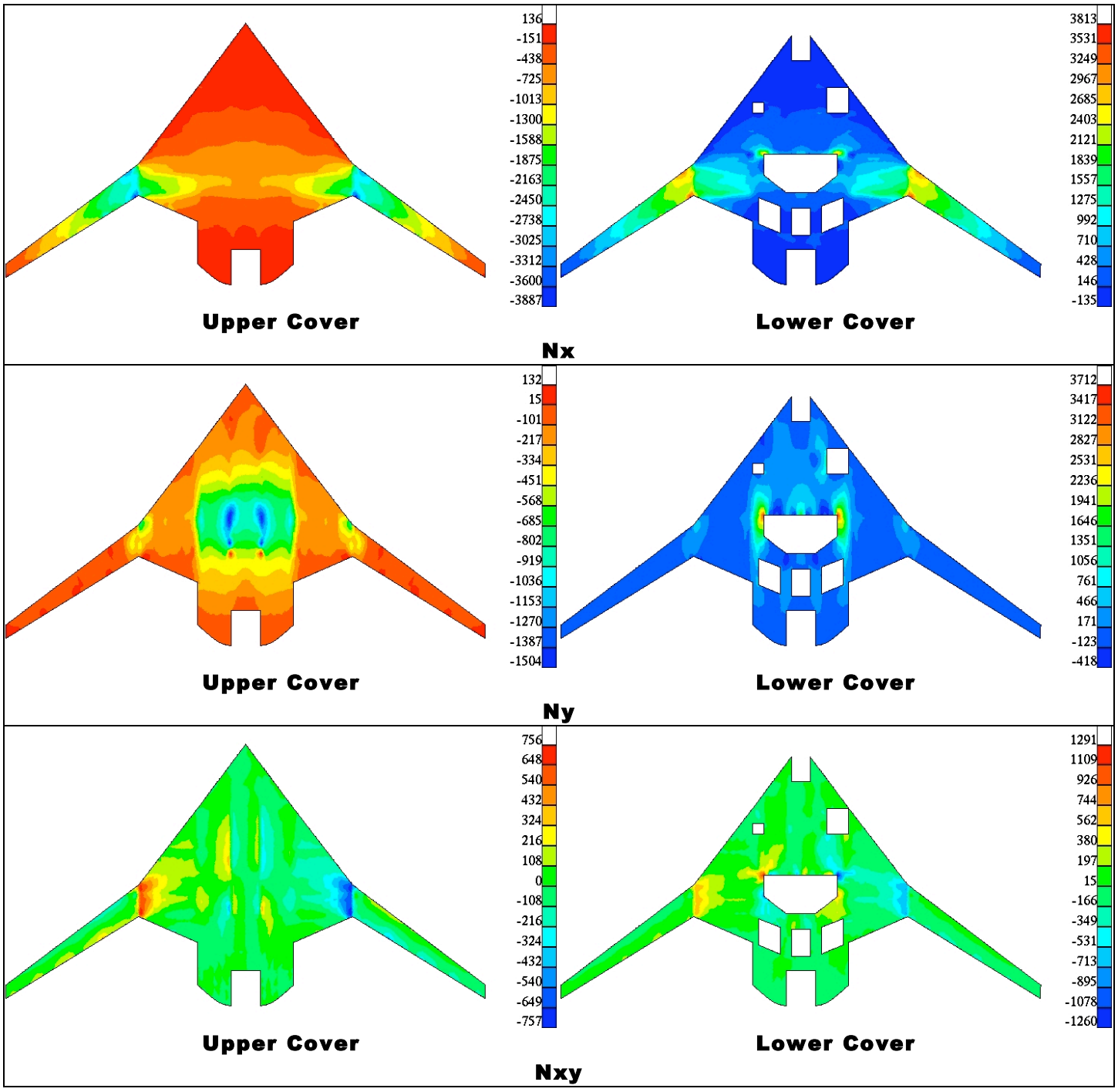

Figure 7: Stress resultants (lbs./in.) for load case 1

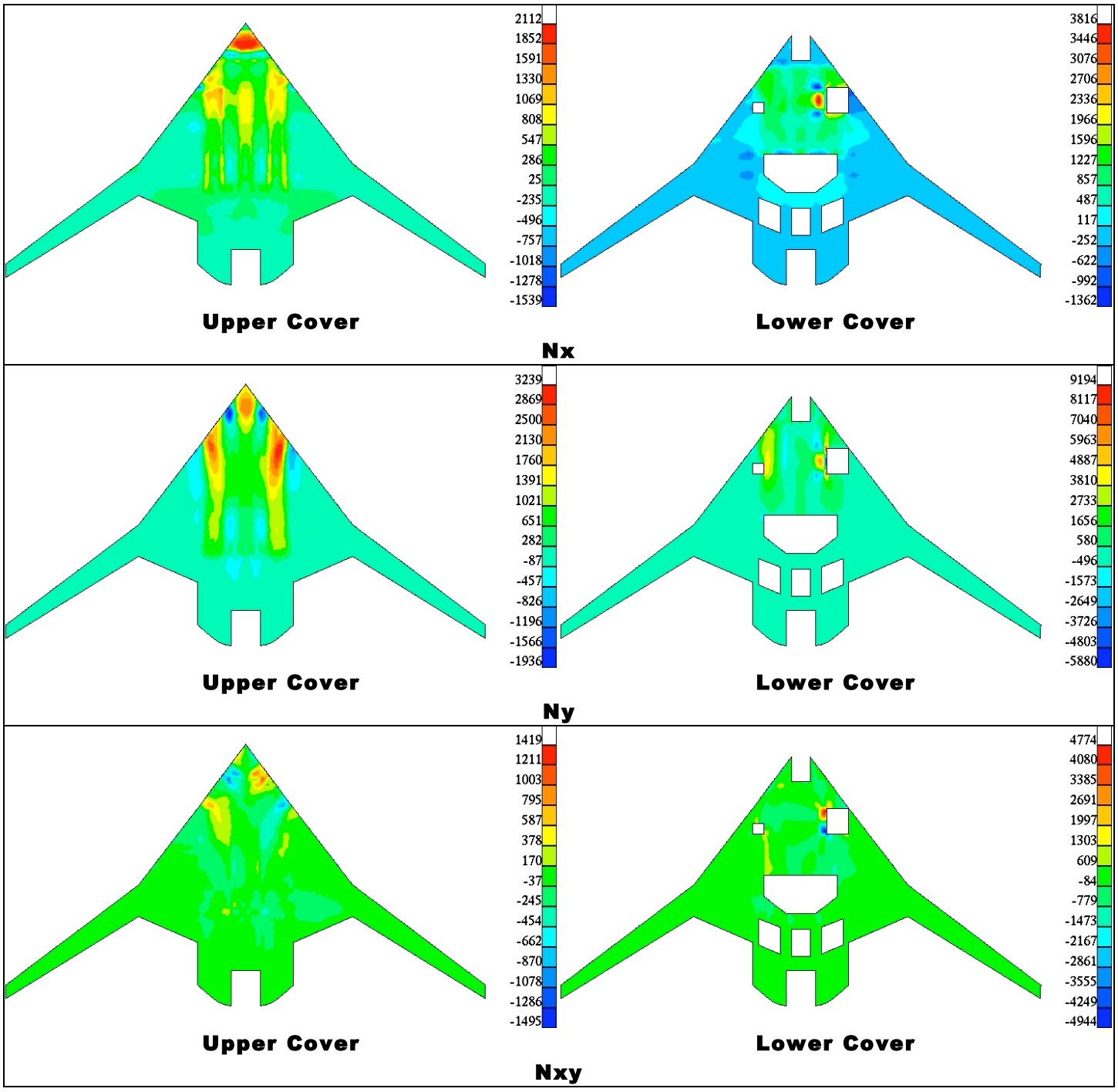

Figure 8: Stress resultants (lbs./in.) for load case 2

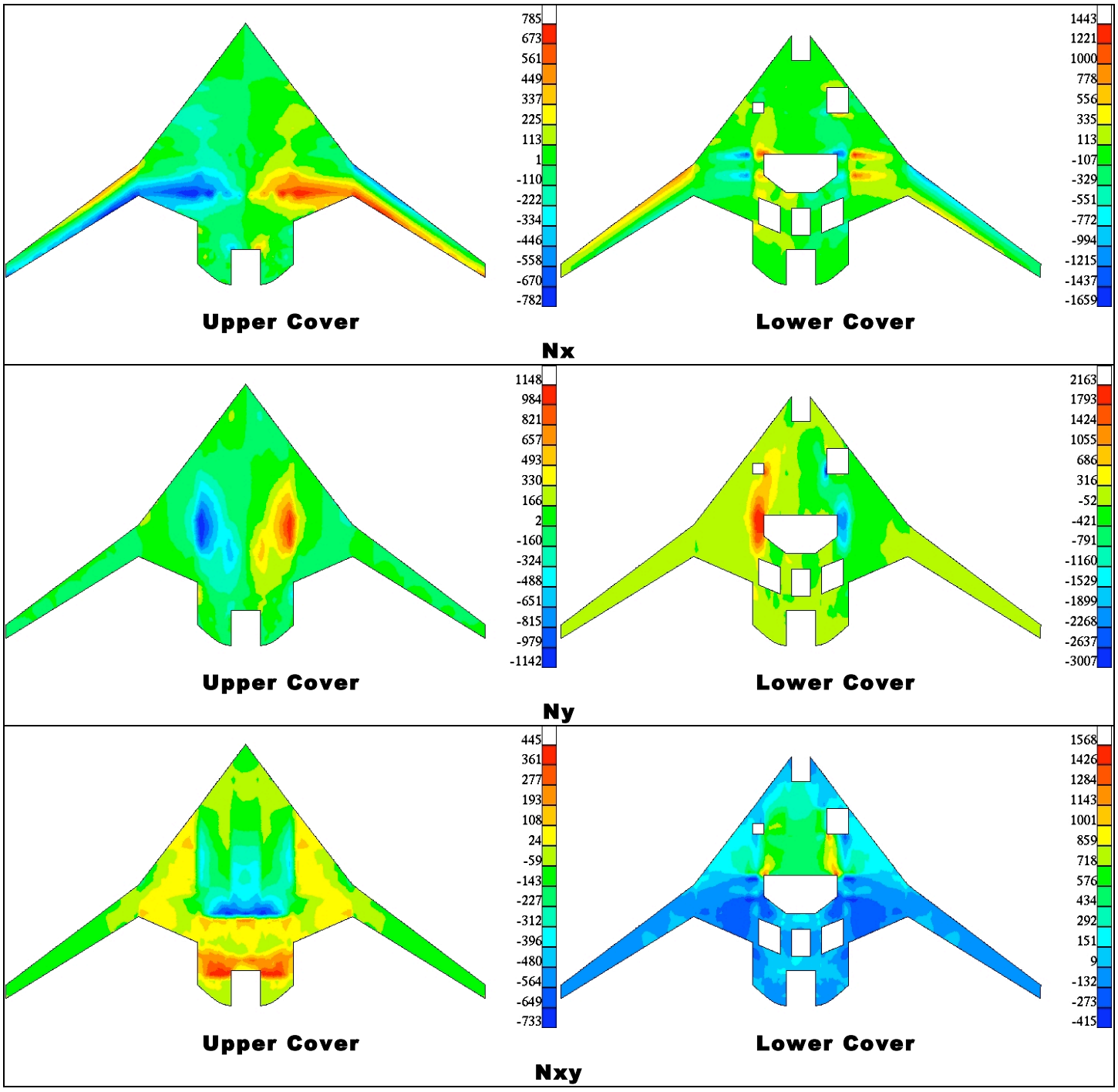

Figure 9: Stress resultants (lbs./in.) for load case 3

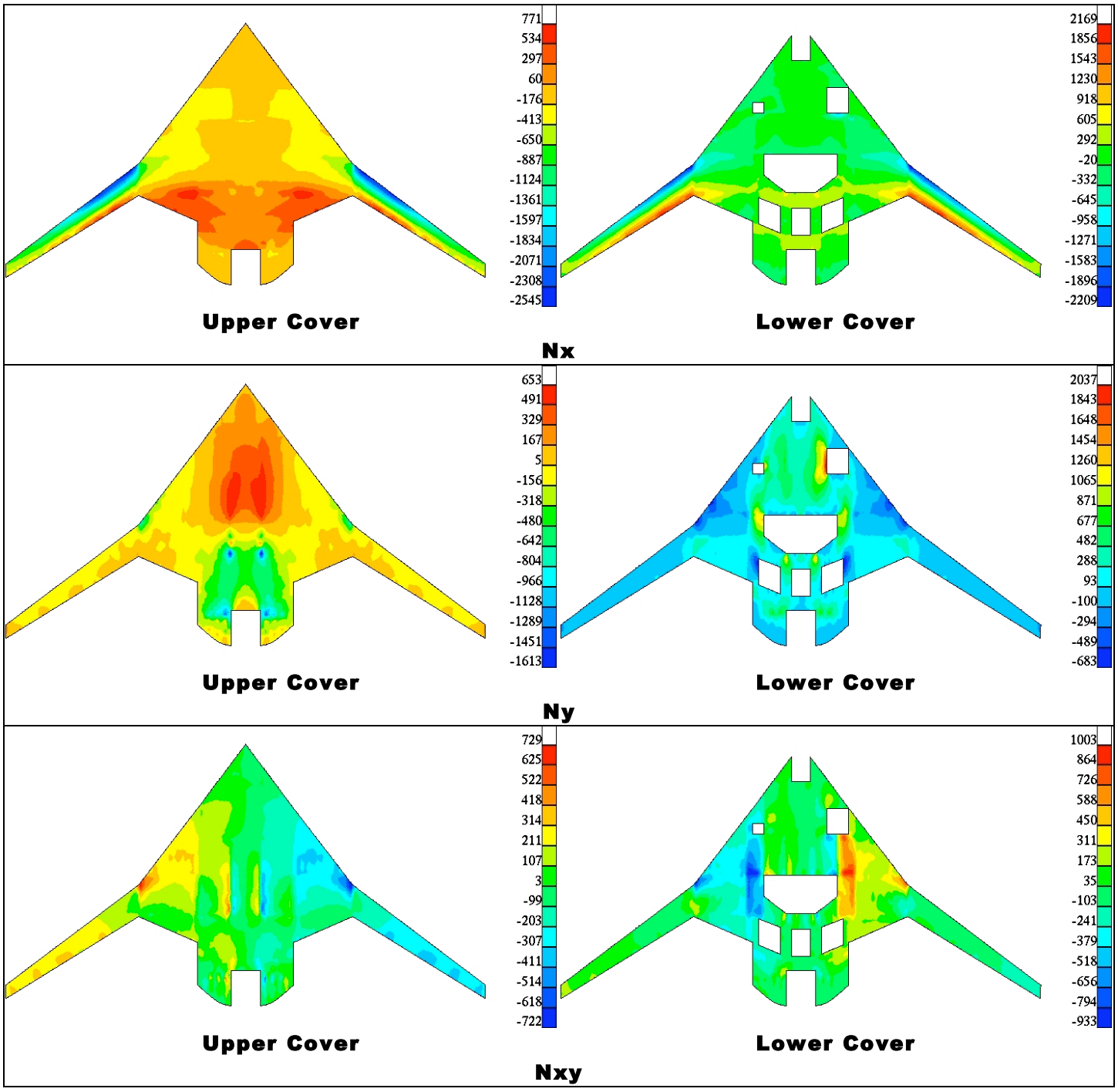

Figure 10: Stress resultants (lbs./in.) for load case 4

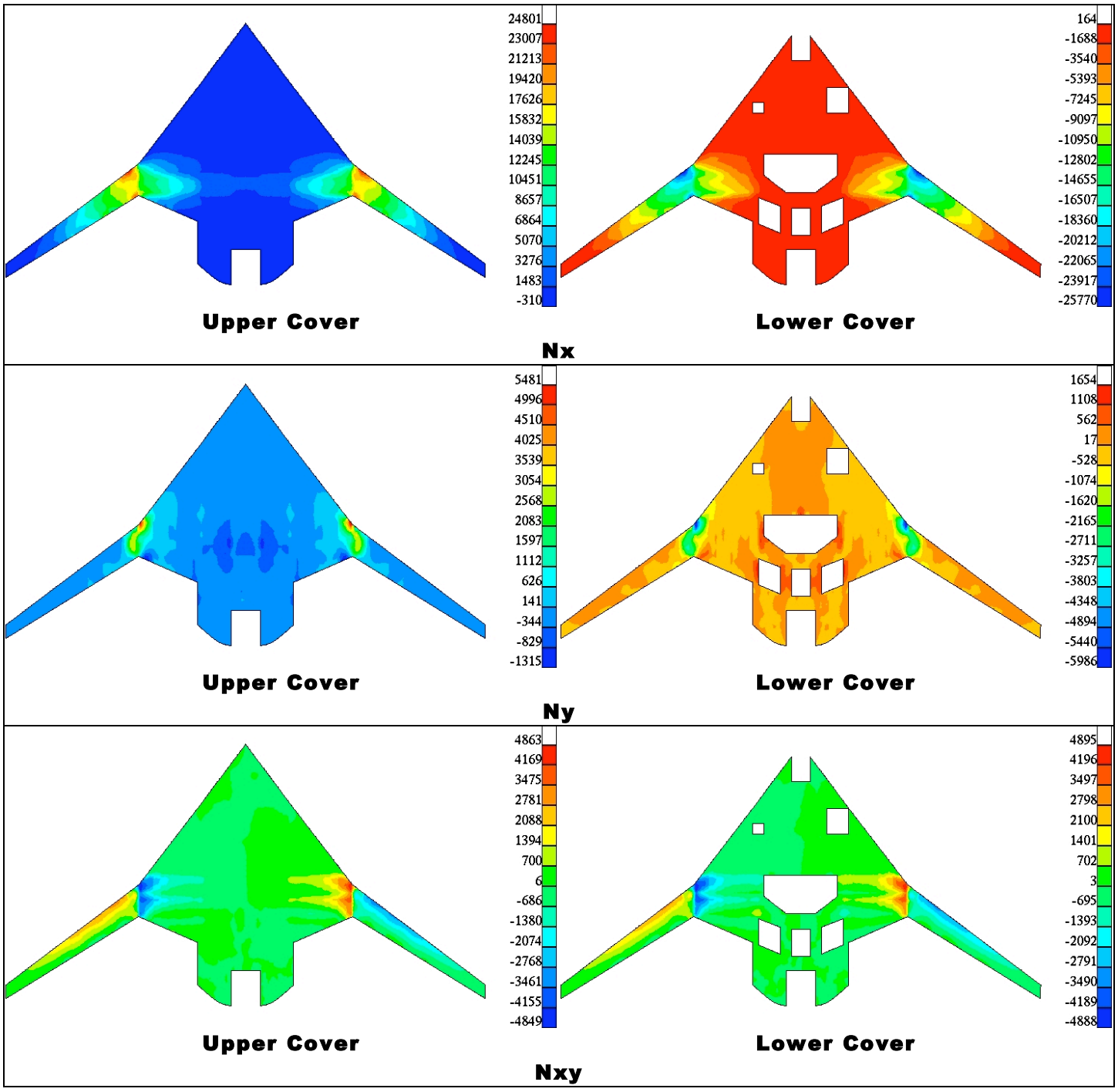

Figure 11: Stress resultants (lbs./in.) for load case 5

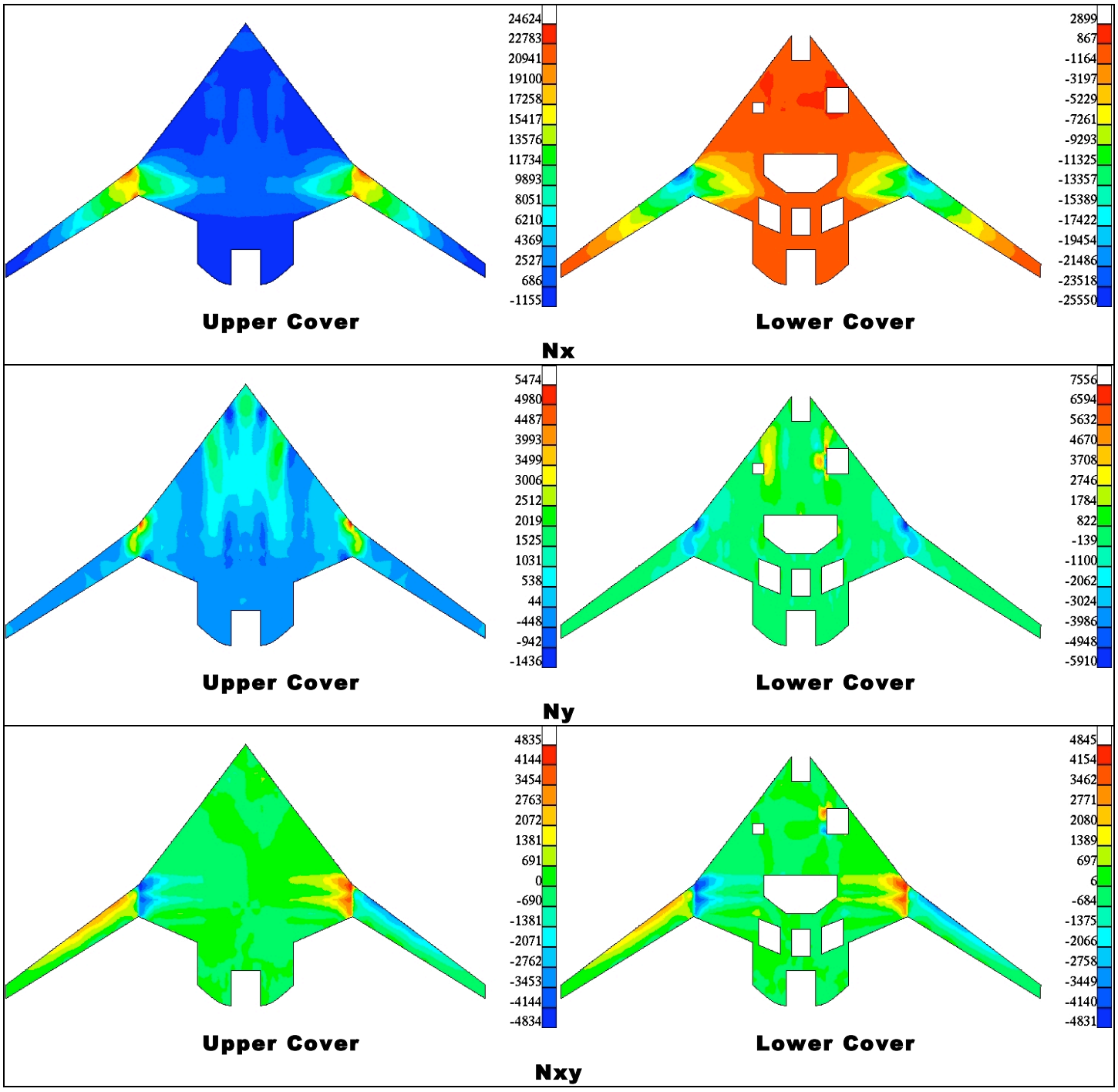

Figure 12: Stress resultants (lbs./in.) for load case 5P

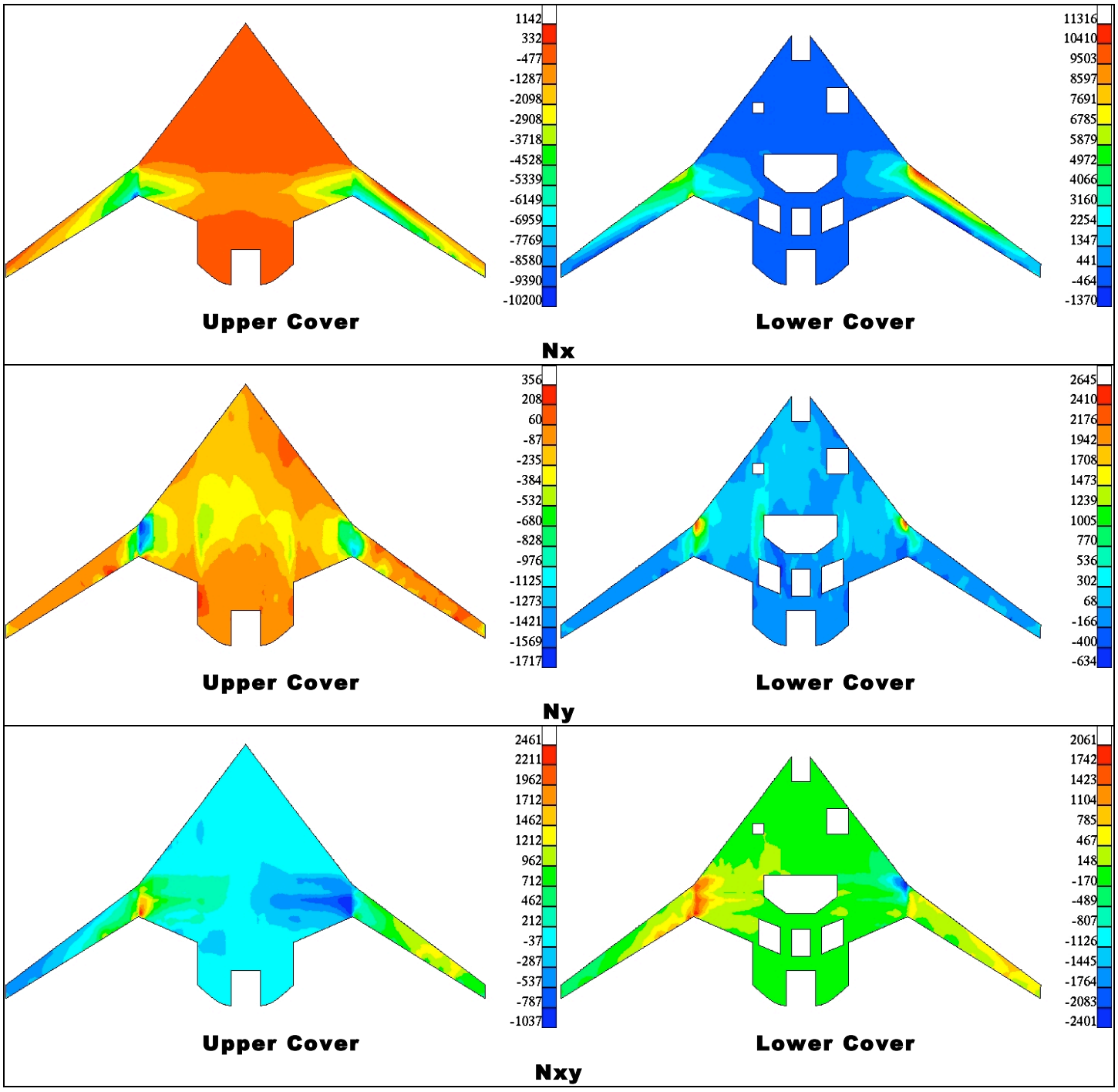

Figure 13: Stress resultants (lbs./in.) for load case 6

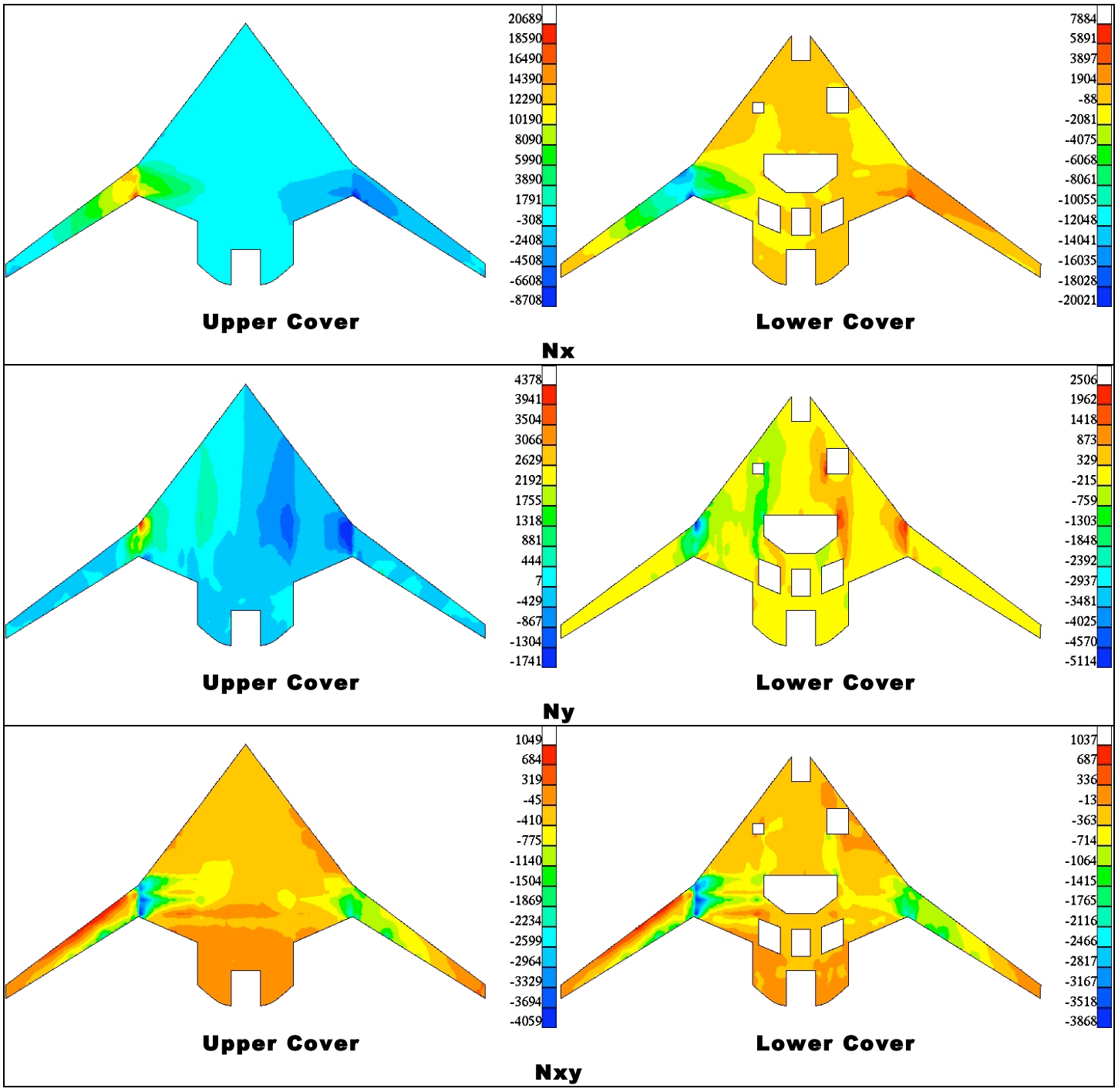

Figure 14: Stress resultants (lbs./in.) for load case 7

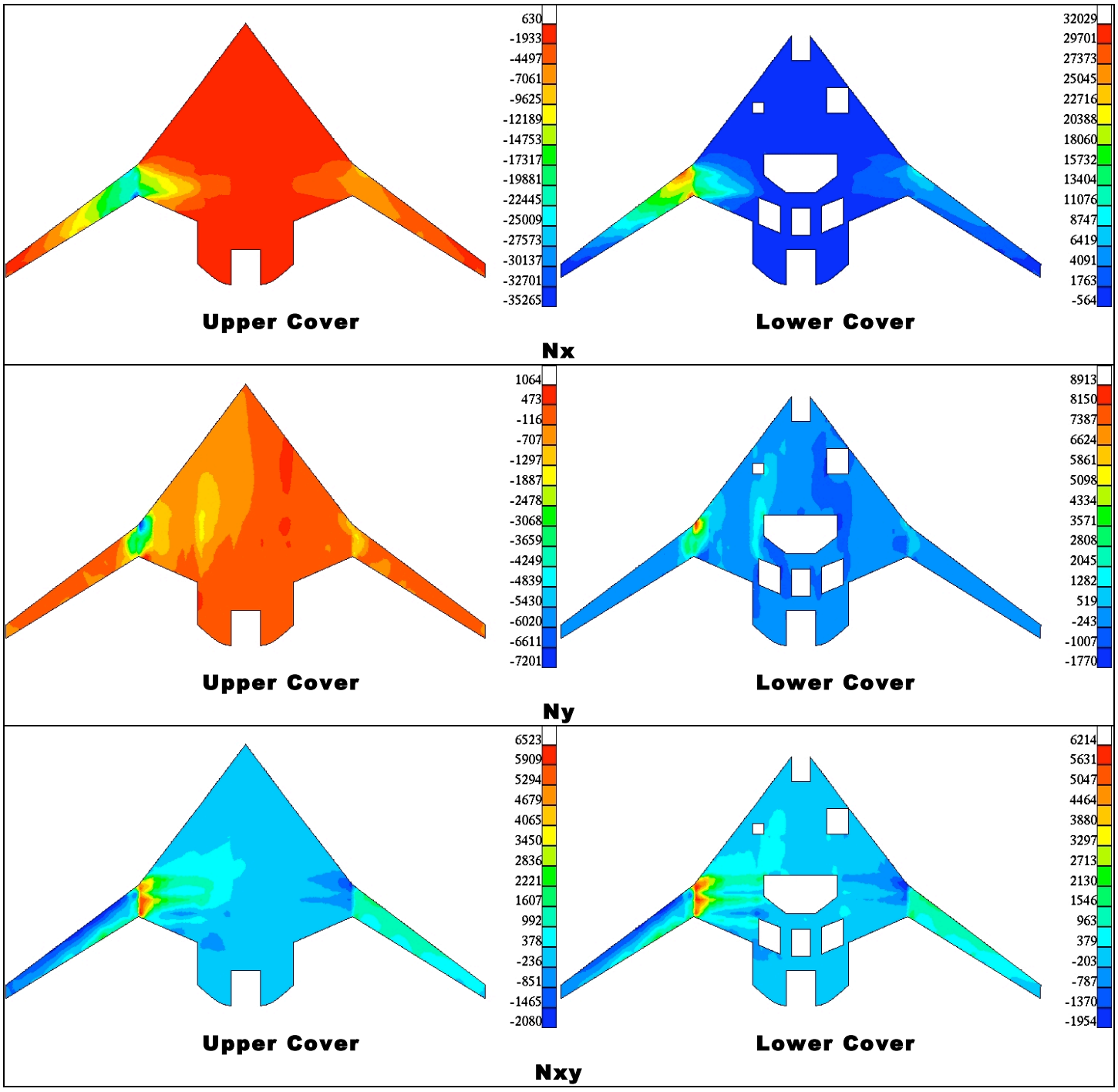

Figure 15: Stress resultants (lbs./in.) for load case 8

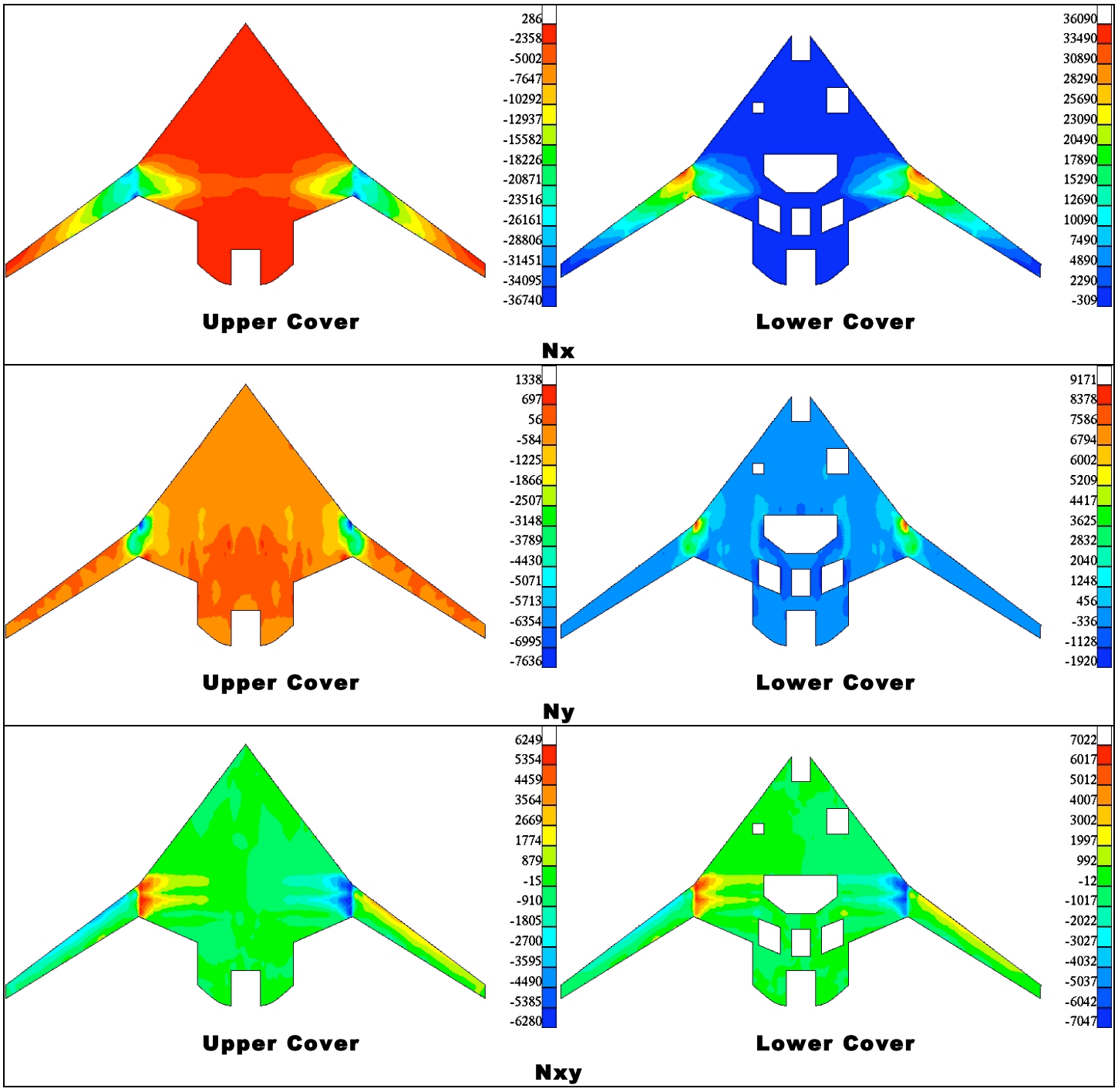

Figure 16: Stress resultants (lbs./in.) for load case 9

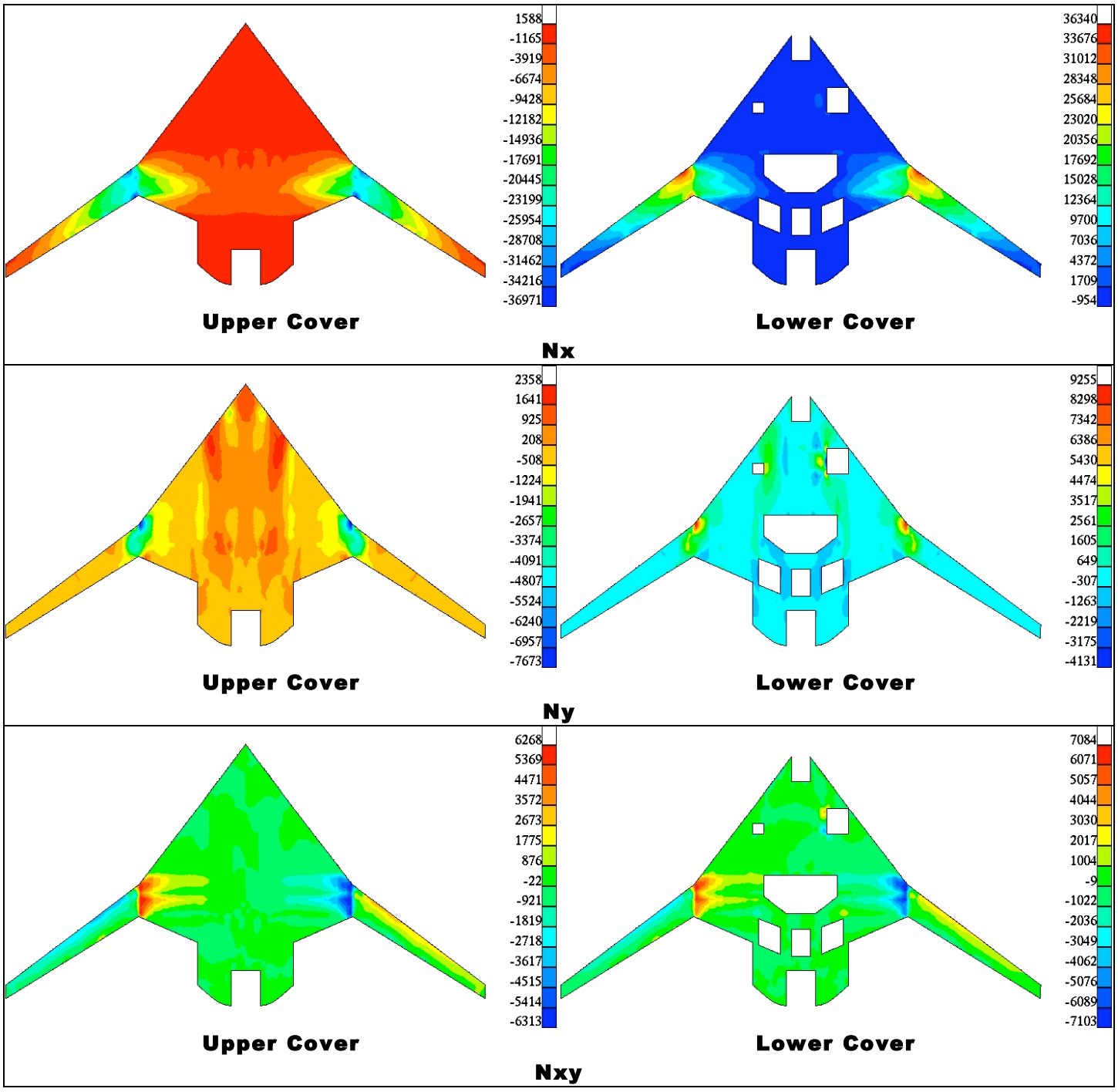

Figure 17: Stress resultants (lbs./in.) for load case 9P

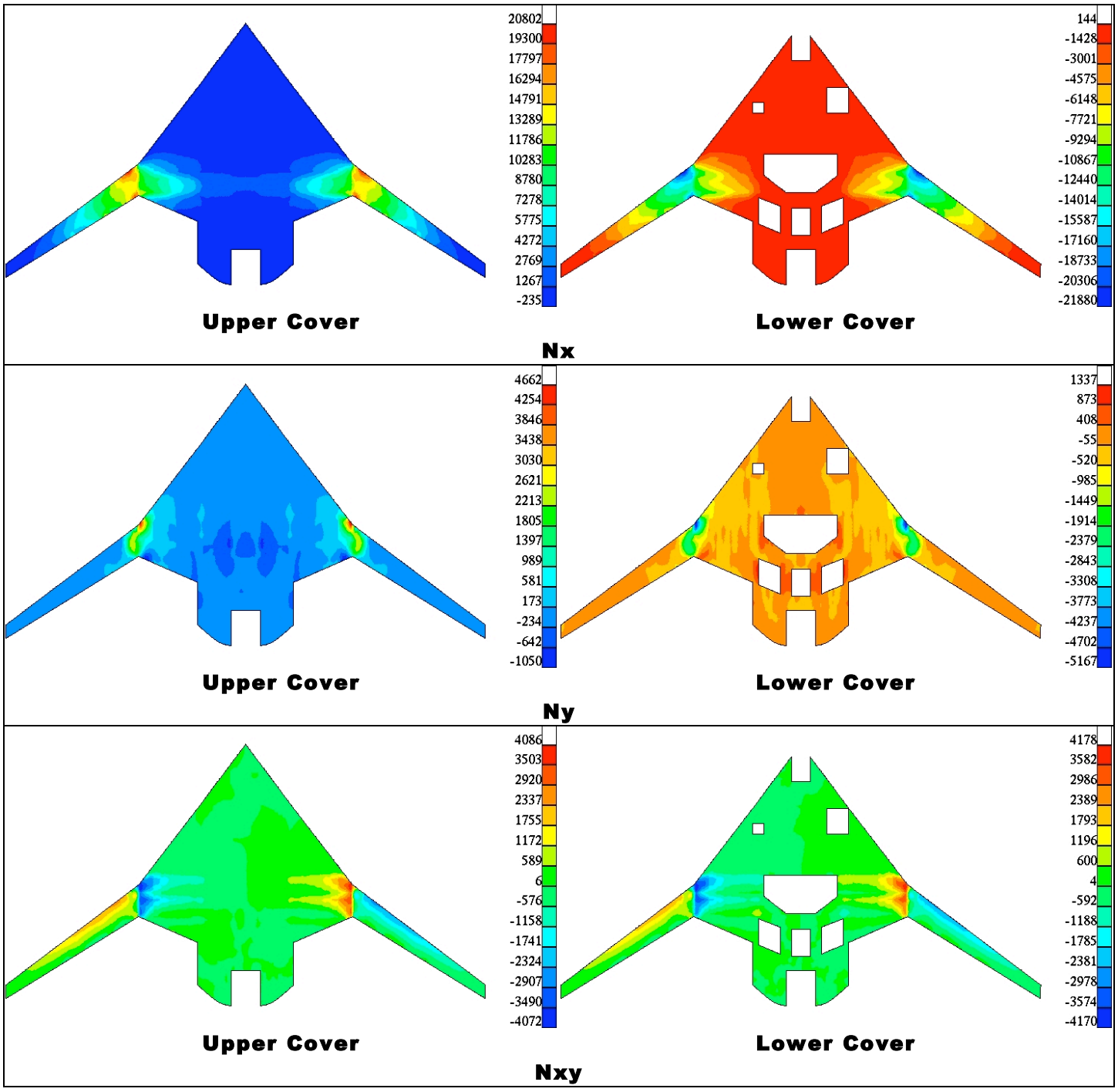

Figure 18: Stress resultants (lbs./in.) for load case 10

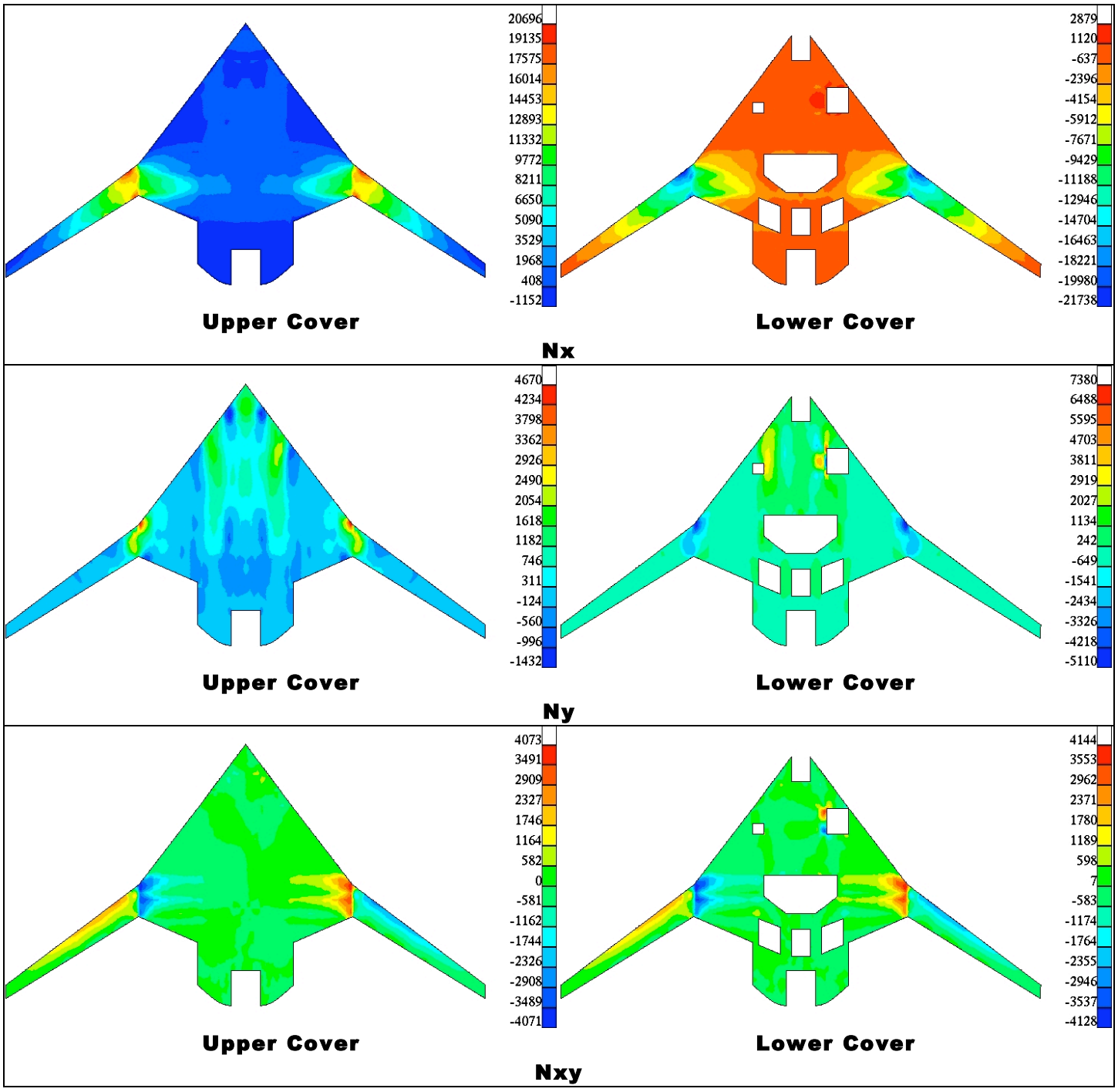

Figure 19: Stress resultants (lbs./in.) for load case 10P

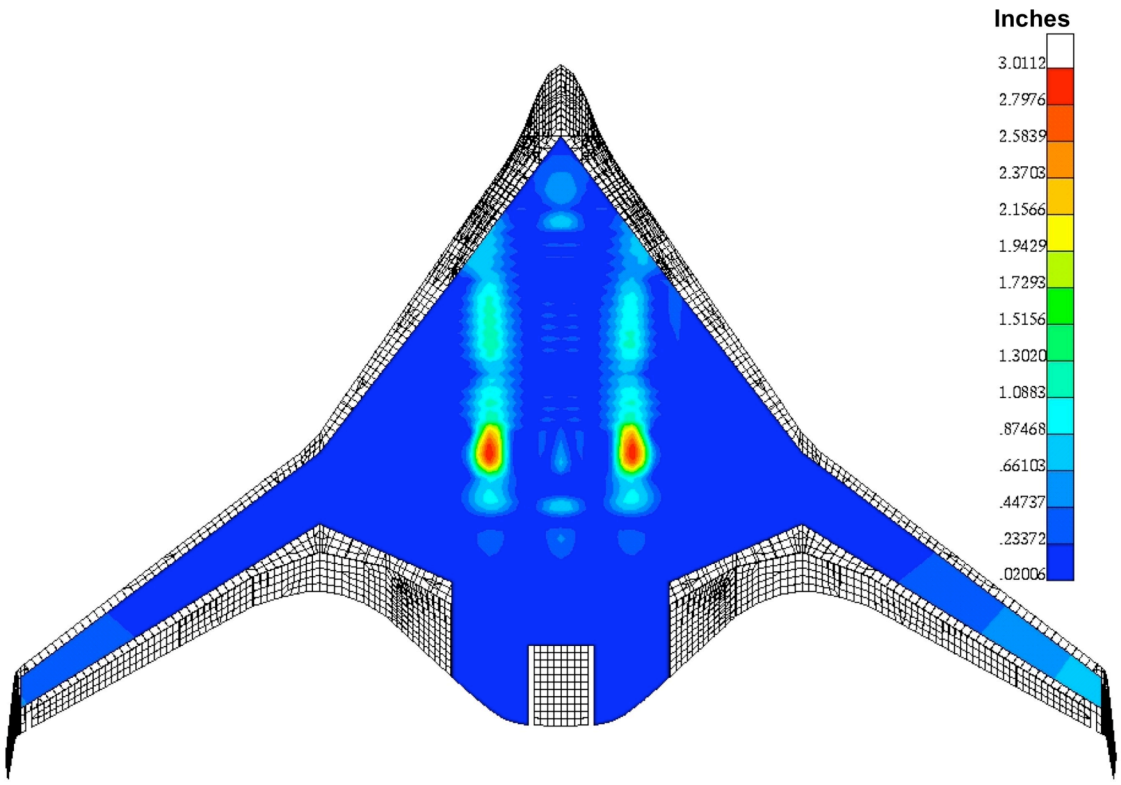

Figure 20: Upper cover deformation differential between load cases 9 and 9P

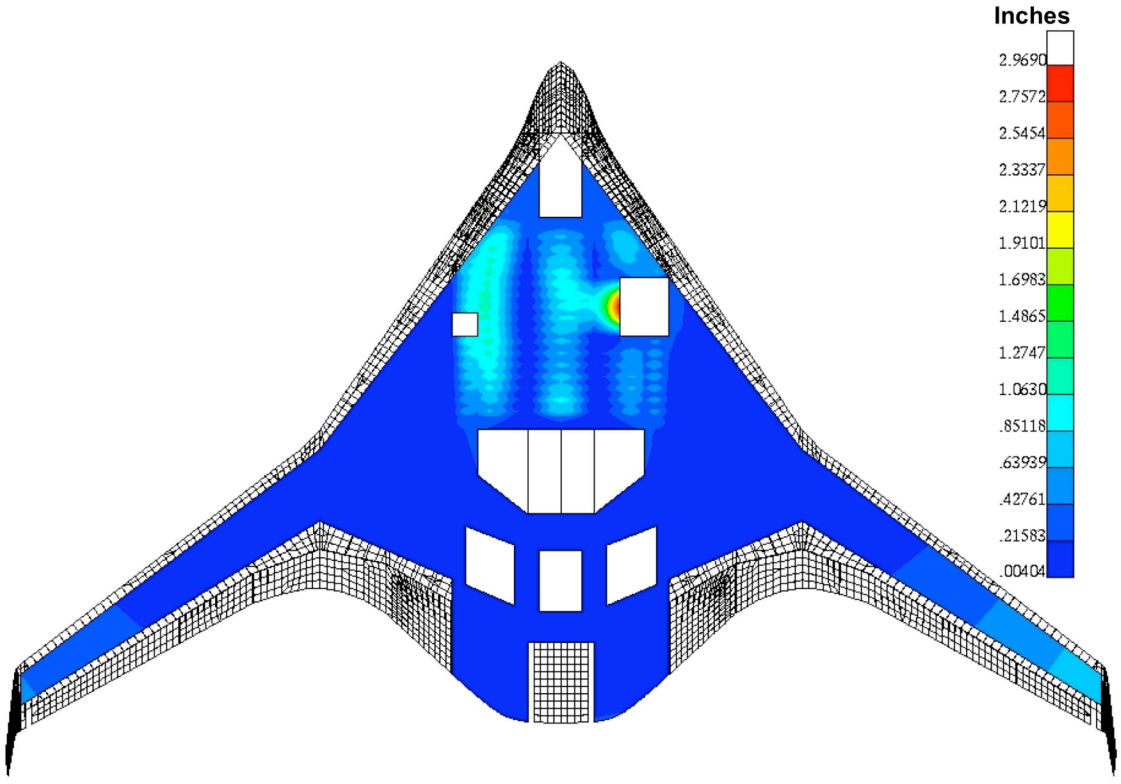

Figure 21: Lower cover deformation differential between load cases 9 and 9P

Region	Section	Cover
1	1 - Inner Wing	Upper
2	1 - Inner Wing	Lower
3	1 - Fuselage	Upper
4	3 - Center Fuse	Lower

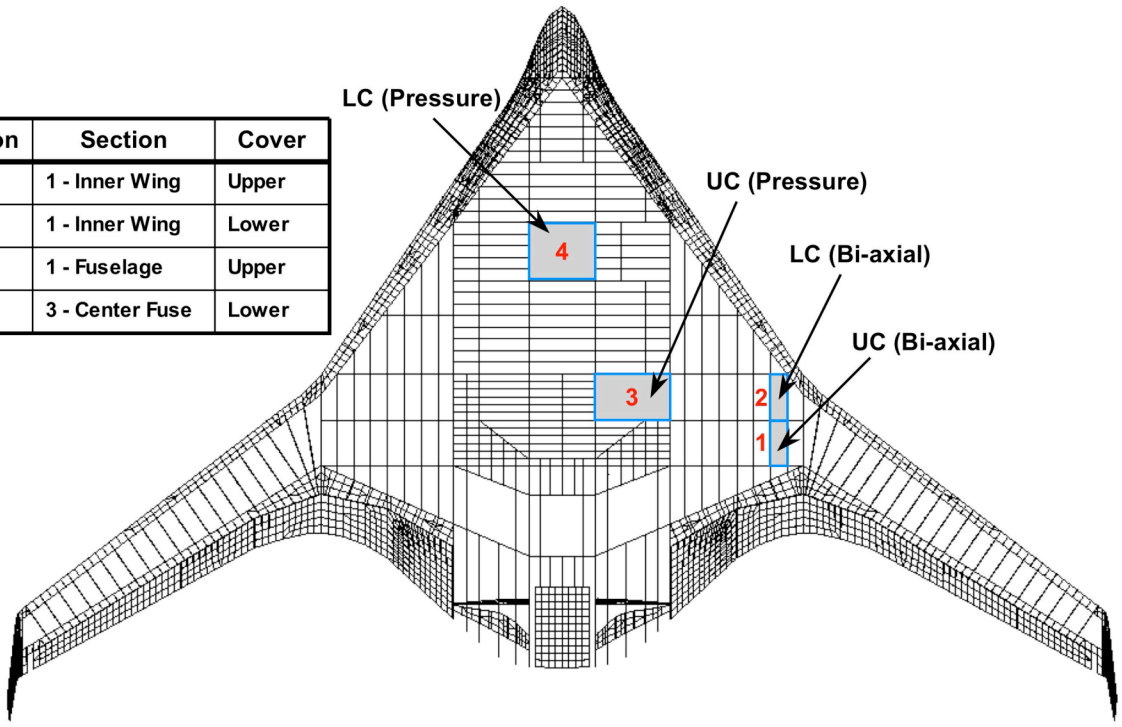

Figure 22: Regions identified for NASA LaRC BWB trade study

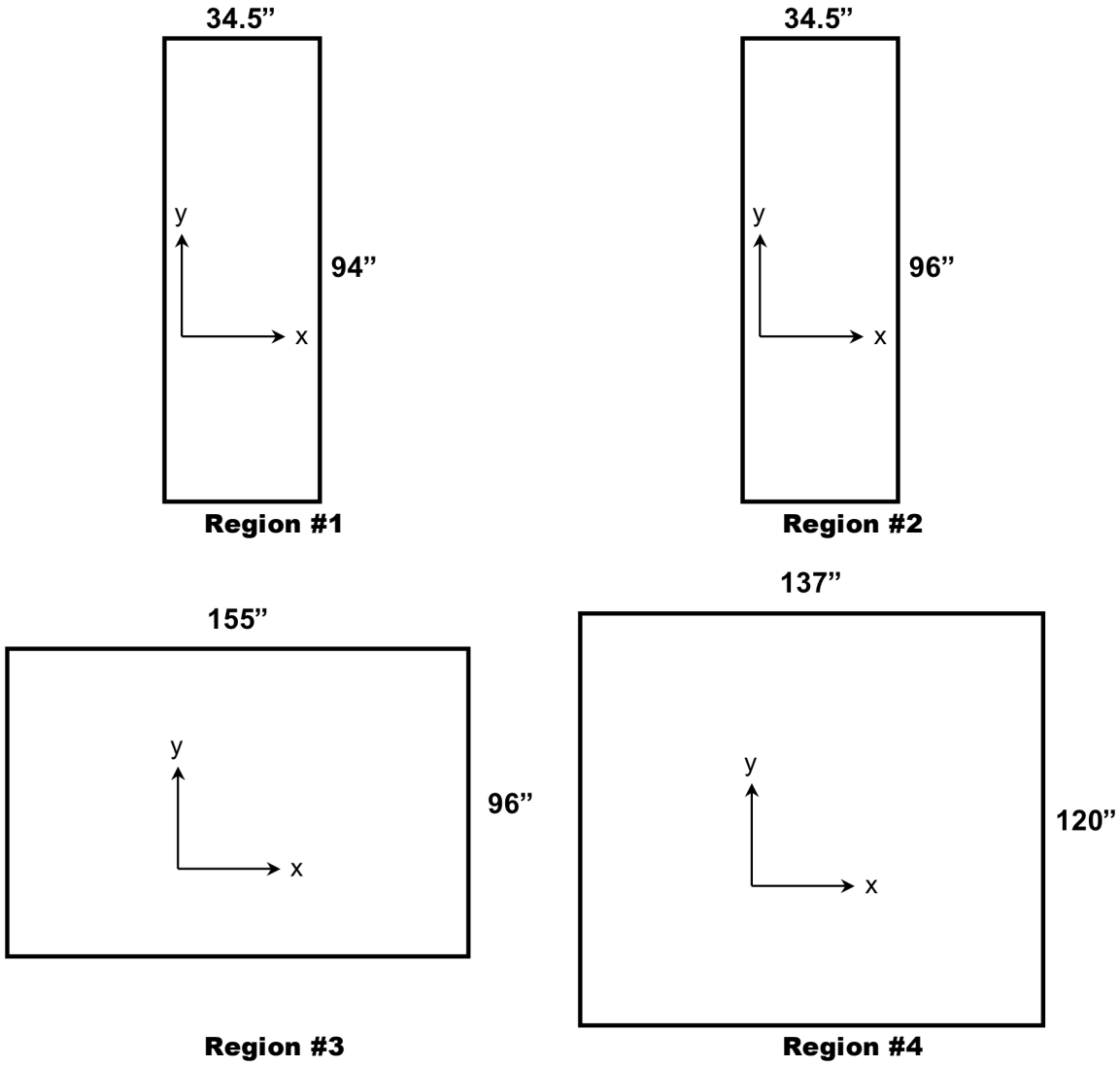

Figure 23: Panel sizes and orientations

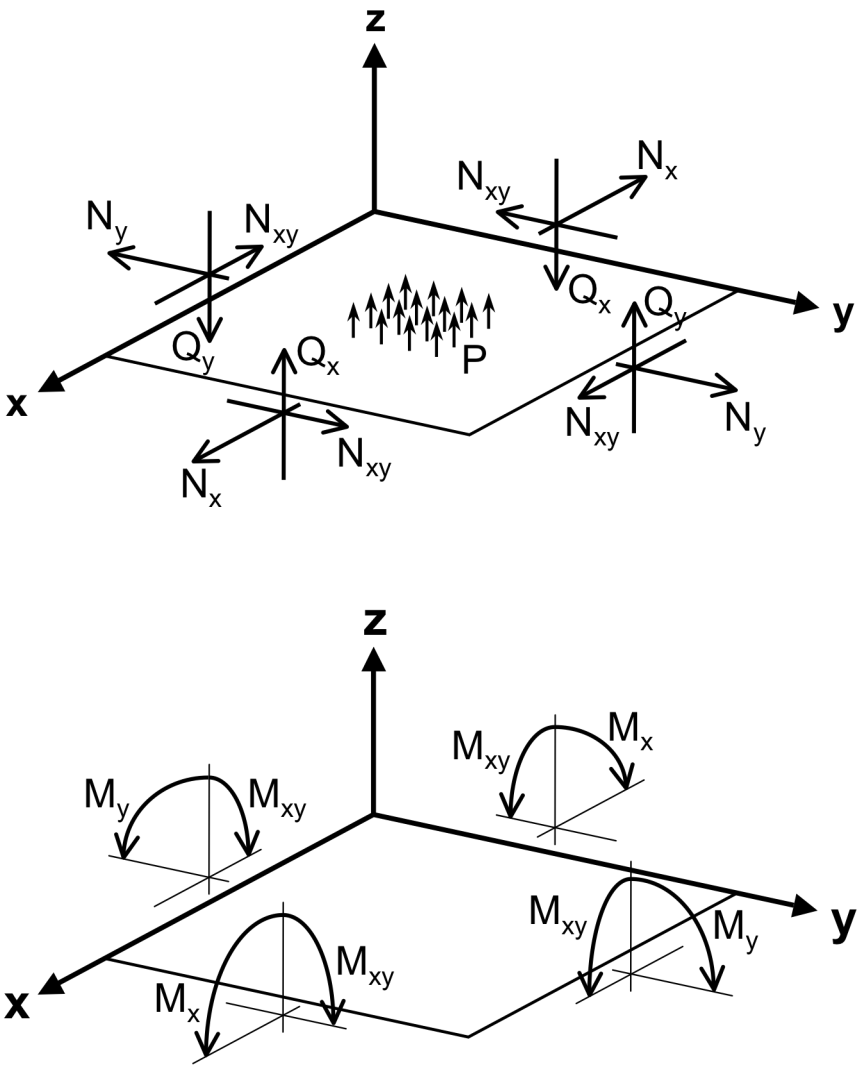

Figure 24: Stress resultant and pressure sign conventions

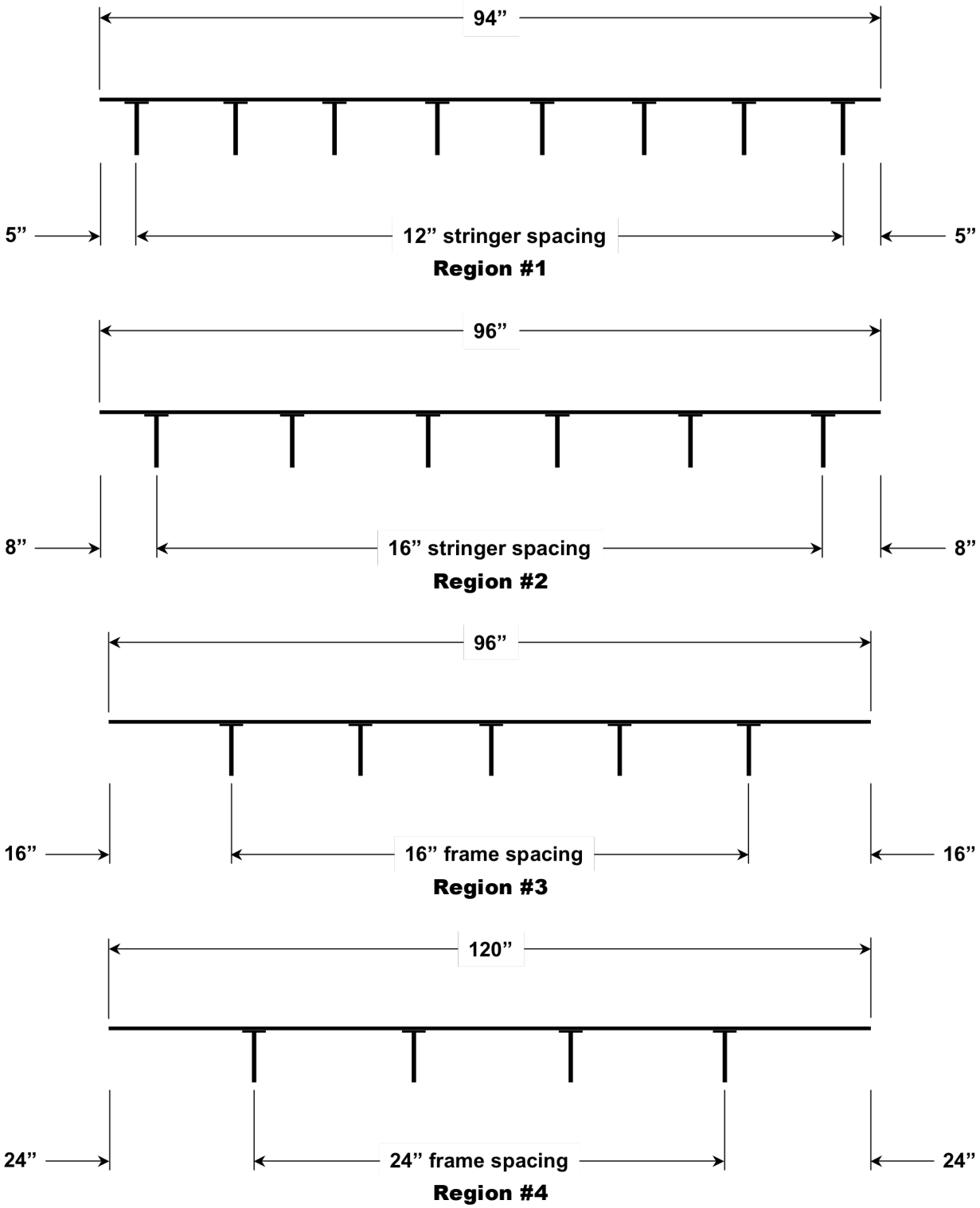

Figure 25: Panel cross-section definitions

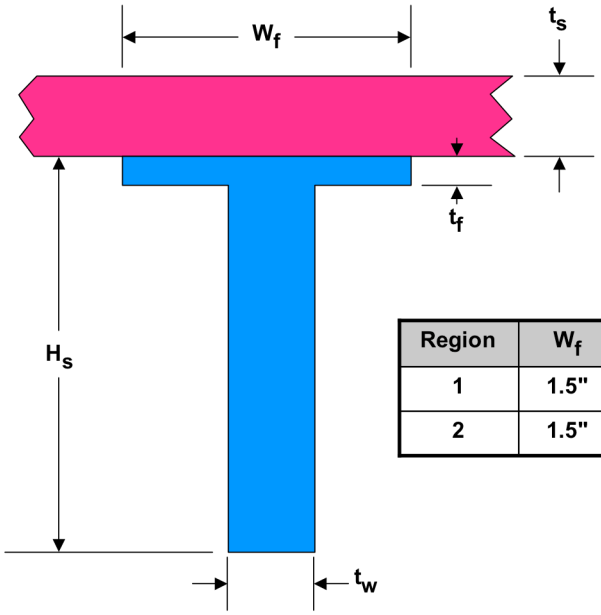

Region	W_f	H_s
1	1.5"	3.3"
2	1.5"	4.7"

Figure 26: Baseline local cross-section for regions 1 and 2

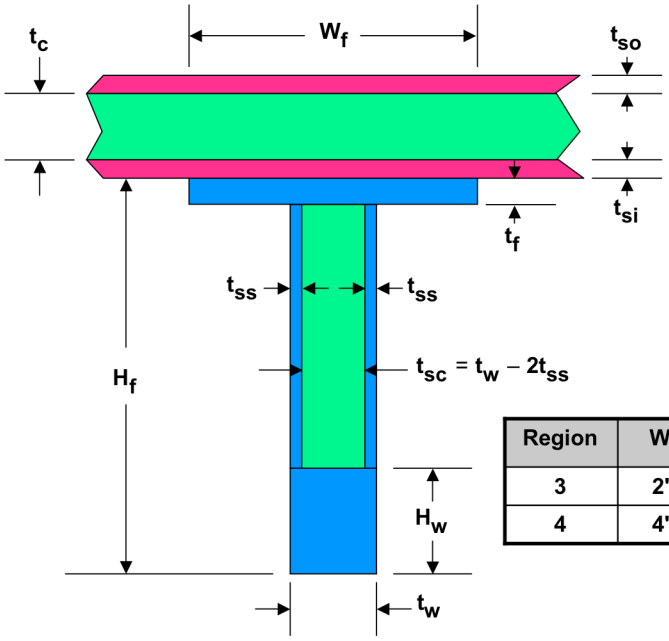

Region	W_f	H_f	H_w
3	2"	5.5"	1.25"
4	4"	5.5"	3"

Figure 27: Baseline local cross-section for regions 3 and 4

Optimization

Trade study regions (see Figure 22 and Table 2) chosen from nonlinear analyses were optimized for the current Boeing BWB baseline panel designs, and used the current BWB baseline panel construction method. Two optimization analysis methods were utilized; 1) MSC/NASTRAN solution 200 [8, 9], and 2) an author-written genetic algorithm (GA). The nonlinear results for the load cases supplied by Boeing were examined, and each region was optimized using the most critical load case for that region (recall Table 3). Constraints were imposed on stress and on buckling. Stresses in the panels representing the trade study regions were examined using the Tsai-Hill failure theory, where the panels studied are assumed to be in plane stress. The Tsai-Hill failure index is defined as:

$$FI = \frac{\sigma_1^2}{X^2} - \frac{\sigma_1\sigma_2}{X^2} + \frac{\sigma_2^2}{Y^2} + \frac{\tau_{12}^2}{S^2}$$

where the failure index, *FI*, was calculated for every ply in every element within the finite element mesh. The values *X*, *Y*, and *S* in the equation are the familiar lamina strengths. When the failure index exceeds unity in any ply, the panel is deemed to have failed. Since the coordinate axes of the panels in the study aligned with the material axes, no stress transformations were required. Failure indices were calculated by specifying the "HILL" option on the PCOMP card in NASTRAN for the solution 200 analyses. The genetic algorithm calculated the failure index using the above equation that was programmed, and was calculated from the centroidal finite element ply stresses.

Originally, constraints on deformations were to be included in the optimization. However, which measure of deformation to use and how to include a measure of aerodynamic importance could not be established. Consider Figure 28, which compares the cross-sections of two possible deformation results (the original cross-section is shown in gray). While the deformation d_2 is almost twice the deformation d_1, d_1 may be far more critical to aerodynamic performance, and could end up being the critical constraint. Therefore, when deflection limits are set and a suitable "aerodynamic deformation" parameter defined, deformation constraints should be included through that parameter.

For optimization, design variables were defined for each trade study region, as shown in Table 6, and these variables were assigned to various property regions of the panels. The property regions are shown in Figures 29 – 32 for the four design regions and represent the skin (larger regions), skin/flange (strip regions) and blades (line between skin/flange regions). A uniform panel is defined as one in which all property regions of the same type are assigned the same design variable (e.g., all skin property sets are assigned the same design variable that represents a skin thickness so that all property sets have the same thickness). Panels of varying thicknesses can be examined by assigning different values of the design variables to each property region. The optimization was then carried out for each of the four trade study regions to minimize panel weight subjected to the stress and buckling constraints. Side constraints on minimum gauge were also included and are provided in Table 7. Initial design variable values (the original baseline design) are provided in Table 8. These original designs represent the starting point for the NASTRAN solution 200 analyses and the baseline chromosomes for the GA analyses. The following sections will discuss the two optimization methods, present the results, and compare the results from these two methods.

Table 6: Trade study region design variable descriptions

Region #	Designation	Description	Included in Property Sets for
1, 2	t_s	Skin thickness	skin, skin/flange
	t_f	Stringer flange thickness	skin/flange
	t_w	Stringer blade thickness	blade
3, 4	t_{si}	Skin inner facesheet thickness	skin, skin/flange
	t_c	Skin core facesheet thickness	skin, skin/flange
	t_{so}	Skin outer facesheet thickness	skin, skin/flange
	t_f	Frame flange thickness	skin/flange
	t_{ss}	Frame sandwich face thickness	frame sandwich
	t_w	Frame web thickness	frame web
	t_{sc}	Frame sandwich core thickness	frame sandwich (calculated)

Table 7: Trade study region design variable maximum and minimum values

Region #	Designation	Minimum Value (in.)	Maximum Value (in.)
1, 2	t_s	0.11 (2 stacks)	2.2 (40 stacks)
	t_f	0.055 (1 stack)	1.1 (20 stacks)
	t_w	0.055 (1 stack)	2.2 (40 stacks)
3, 4	t_{si}	0.055 (1 stack)	0.55 (10 stacks)
	t_c	0.05	4.0
	t_{so}	0.11 (2 stacks)	1.1 (20 stacks)
	t_f	0.055 (1 stack)	1.1 (20 stacks)
	t_{ss}	0.055 (1 stack)	0.11 (2 stacks)
	t_w	0.275 (5 stacks)	2.2 (40 stacks)
	t_{sc}	0.055 (calculated)	2.09 (calculated)

Table 8: Original trade study region design variable values

Region #	Designation	Value (in.)	Baseline Weight (lbs.)
1	t_s	0.715 (13 stacks)	
	t_f	0.055 (1 stack)	153.4
	t_w	0.385 (7 stacks)	
2	t_s	0.55 (10 stacks)	
	t_f	0.055 (1 stack)	120.1
	t_w	0.275 (5 stacks)	
3	t_{so}	0.055 (1 stack)	
	t_c	0.35	
	t_{si}	0.11 (2 stacks)	
	t_f	0.515 (~9 stacks)	299.7
	t_{ss}	0.055 (1 stack)	
	t_w	1.0 (~18 stacks)	
	t_{sc}	0.89	
4	t_{so}	0.055 (1 stack)	
	t_c	0.35	
	t_{si}	0.11 (2 stacks)	
	t_f	0.515 (~9 stacks)	362.4
	t_{ss}	0.055 (1 stack)	
	t_w	1.0 (~18 stacks)	
	t_{sc}	0.89	

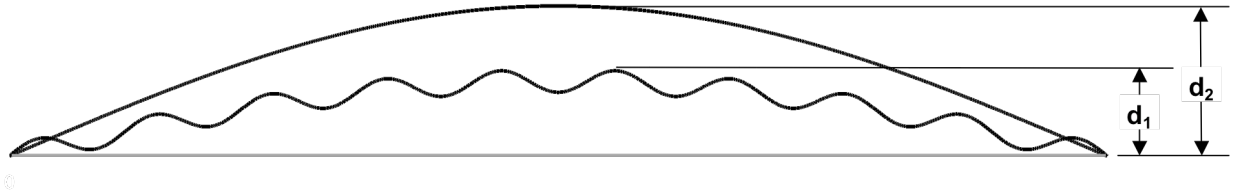

Figure 28: Deformation comparison for constraint generation

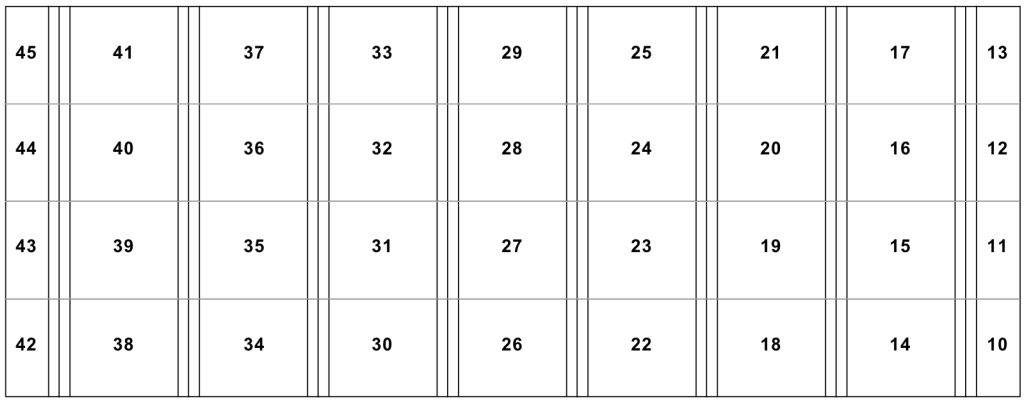

Skin

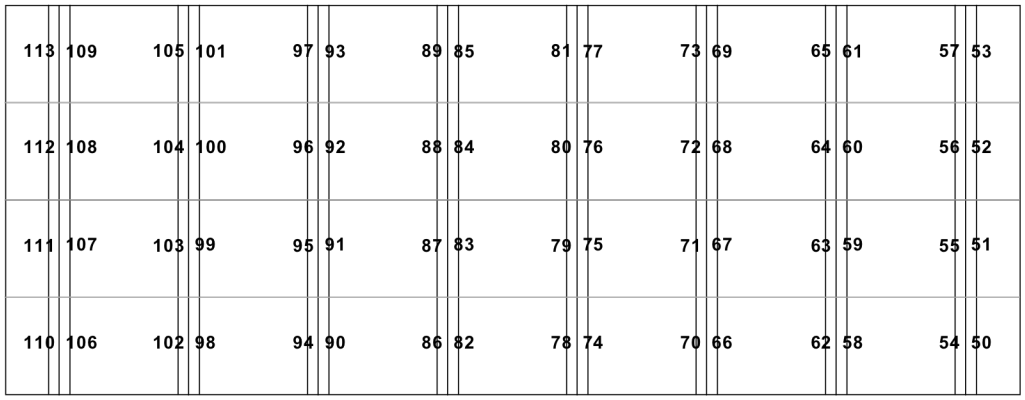

Skin/Flange

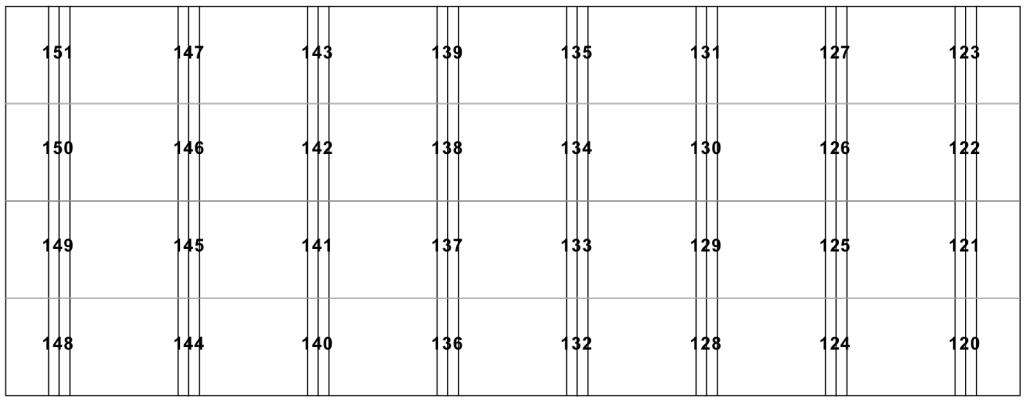

Blade

Figure 29: Property set regions and numbers for region 1 panel

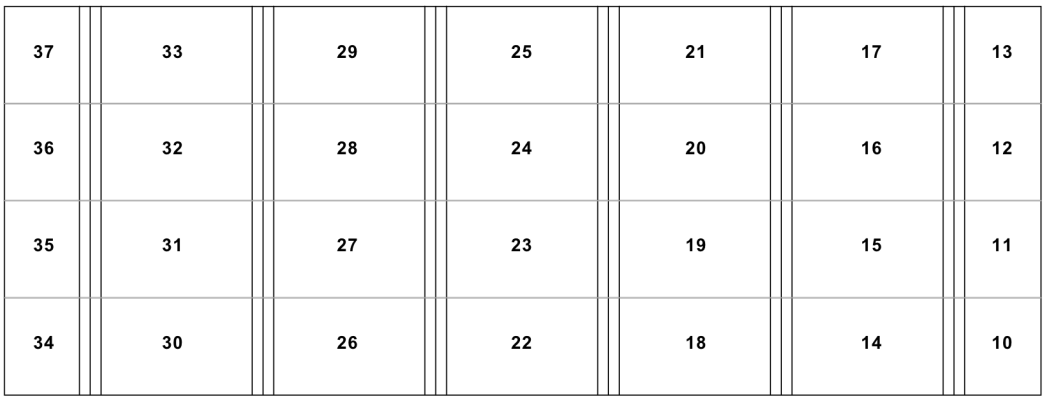

Figure 30: Property set regions and numbers for region 2 panel

50	51	52	53	54	55	56	57
42	43	44	45	46	47	48	49
34	35	36	37	38	39	40	41
26	27	28	29	30	31	32	33
18	19	20	21	22	23	24	25
10	11	12	13	14	15	16	17

Skin

188	189	190	191	192	193	194	195
180	181	182	183	184	185	186	187
172	173	174	175	176	177	178	179
164	165	166	167	168	169	170	171
156	157	158	159	160	161	162	163
148	149	150	151	152	153	154	155
140	141	142	143	144	145	146	147
132	133	134	135	136	137	138	139
124	125	126	127	128	129	130	131
116	117	118	119	120	121	122	123
108	109	110	111	112	113	114	115
100	101	102	103	104	105	106	107

Skin/Flange

232	233	234	235	236	237	238	239
224	225	226	227	228	229	230	231
216	217	218	219	220	221	222	223
208	209	210	211	212	213	214	215
200	201	202	203	204	205	206	207

Blade (add 100 for frame sandwich portion property ID)

Figure 31: Property set regions and numbers for region 3 panel

42	43	44	45	46	47	48	49
34	35	36	37	38	39	40	41
26	27	28	29	30	31	32	33
18	19	20	21	22	23	24	25
10	11	12	13	14	15	16	17

Skin

172	173	174	175	176	177	178	179
164	165	166	167	168	169	170	171
156	157	158	159	160	161	162	163
148	149	150	151	152	153	154	155
140	141	142	143	144	145	146	147
132	133	134	135	136	137	138	139
124	125	126	127	128	129	130	131
116	117	118	119	120	121	122	123
108	109	110	111	112	113	114	115
100	101	102	103	104	105	106	107

Skin/Flange

224	225	226	227	228	229	230	231
216	217	218	219	220	221	222	223
208	209	210	211	212	213	214	215
200	201	202	203	204	205	206	207

Blade (add 100 for frame sandwich portion property ID)

Figure 32: Property set regions and numbers for region 4 panel

NASTRAN Solution 200

Solution 200 (DESOPT) is the design optimization solution in MSC/NASTRAN [9]. The optimization solution uses the results from various NASTRAN analysis solutions that are specified in separate subcases [9]. For the current optimization study, only the static and buckling analyses are utilized. The optimizer is specified by the user and can be the default optimizer, DOT [10] which is licensed from Vanderplaats Research and Development, Inc., or the ADS optimizer [11] that was enhanced by MSC. Sensitivities required for the optimization are calculated explicitly wherever possible, but when calculation of these sensitivities is not practical, NASTRAN utilizes finite differences (forward or central). Several gradient-based methods are available for the optimizers, and References 8 and 9 provide details about optimizer methods and selection. The general procedure is for NASTRAN to conduct an optimization using continuous design variables. However, it is possible to make some or all of the design variables discrete. If any of the design variables are discrete, NASTRAN performs the optimization with continuous variables, then chooses the discrete variables based upon the continuous solution for a final optimization. The method NASTRAN uses to process the discrete variables is specified by the DISCOD parameter in the DOPTPRM command, the default being design of experiments. The current optimization study examines using both continuous and discrete design variables in the NASTRAN analyses.

PATRAN was used to generate the finite element models for the four trade study regions. Finite element meshes comprised CQUAD4 elements as shown in Figures 33 – 36. Properties for the shell elements were assigned using the composite laminate (PCOMP) formulation. Since offsets are not permitted in the NASTRAN buckling analysis, it was necessary to create dummy plies on both surfaces of the laminates. Figure 37 demonstrates the use of a single dummy ply when a three-ply laminate is positioned with the outer surface at the outer mold line (OML), which is also the nodal surface. In this case, the original offset, ZOFFS, would be equal to half of the thickness of the total laminate and be negative because the direction from the nodal surface to the reference surface is opposite from the element normal direction (Figure 37a). To eliminate this offset, the dummy ply is added to the outer surface with a thickness equal to the total laminate, resulting in zero offset (ZOFFS = 0) (Figure 37b). The dummy ply is assigned a material having negligible property values, so that the dummy ply has no true effect on the overall stiffness. The dummy plies are given an initial nominal thickness of 0.0001 inches in the baseline design, are then adjusted when structural thicknesses are modified so that the resulting laminate property will have no offset. For example, consider a skin property that originally has a thickness of 0.5 inches. A laminate with three plies having thicknesses of 0.0001, 0.5 and 0.0001 inches, respectively, is created and no offset is assigned (this is equivalent to a coincident nodal surface and reference surface). Then, if the skin thickness is changed to 0.4 inches, the property is modified to have thicknesses of 0.1001, 0.4 and 0.0001 inches, respectively, and still has no assigned offset.

Buckling analyses were carried out for the four regions. Fundamental buckling load factors and modes are provided in Figures 38 and 39 for regions 1 and 3, respectively. The buckling mode for region 1 is essentially a local panel buckling mode between stringers. Design criteria provided allows for local panel buckling, between stringers and frames, at a load factor of 0.35. Therefore, the buckling constraint for the optimization was set equal to 0.35 for region 1. Region 3 demonstrates a more global buckling response in that it includes the frames. Figure 40 shows the deformation in the vicinity of region 3, where it is clearly seen that the deformation is inclusive of the frames, and is a global response. Design criteria provided allows global buckling at a load factor of 1.0. Therefore, the buckling constraint for the optimization was set equal to 1.0 for region 3. Buckling was not significant (large load factor values) for regions 2 and 4, so plots of the fundamental mode for these regions are not included. The buckling constraints for the optimization of regions 2 and 4 were set to the values for regions 1 and 3, respectively, but had no real effect on the solution.

Region 1 was optimized using four separate NASTRAN solution 200 analyses. The design variables, type and assigned property identification numbers (IDs) for these four analyses are provided in Table 9. Property IDs referenced in the table refer to those defined in Figure 29. The first two analyses (R1-1 and R1-2) for a panel with uniform skin, the panel most easily manufactured. Analyses R1-1 and R1-2

utilized all continuous and all discrete variables, respectively. All property sets associated with a particular part of the panel (skin, skin/flange or stringer blade) were assigned using the same three design variables. The core thickness increment, when it was treated as a discrete design variable, was equal to the minimum value chosen for the study, 0.05 inches. Analyses R1-3 and R1-4 permit the skin thickness in the skin/flange property sets to differ from the skin thickness in the skin only property sets. Again, property sets of particular panel parts were assigned the same design variables. Additional analyses were attempted where each property set was assigned independent design variables, but convergence was not satisfactory and the resulting solution was not realistic or practical. Thus, the optimization analyses for all four regions were limited to a small number of design variables. Additional discussion of the problems encountered with a large number of design variables is presented later in this report. Results for the four region 1 NASTRAN optimization analyses are presented in Table 10. The four analyses suggest panels whose weights are significantly larger than the baseline weight shown in Table 8. All four analyses were buckling critical, that is, the buckling constraint was active and drove the solution. Figure 41 shows the fundamental buckling mode shape for the R1-3 optimization analysis. Mode shapes are similar for the other region 1 analyses.

Region 2 was also optimized using four separate NASTRAN solution 200 analyses. The design variables, type and assigned property IDs for these four analyses are provided in Table 11. Property IDs referenced in the table refer to those defined in Figure 30. The region 2 optimization analyses are defined consistent with those for region 1. Thus, analyses R2-1 and R2-2 have three design variables, and analyses R2-3 and R2-4 have four design variables. The results for the region 2 NASTRAN optimization analyses are presented in Table 12. Note in the table that the failure index for analysis R2-2 is significantly less than unity. This is due to the fact that R2-2 is the discrete variable solution that arises from analysis R2-1, where the values for the continuous variables are replaced by discrete values. In this case, the thickness of the stringer blade, which is represented by variable 3, is increased from 0.13515 to 0.165 inches. Since the stringer blade is the portion of the panel having the maximum failure index, the maximum failure index for the panel decreases significantly. Conversely, the thickness of the stringer blade in analysis R2-4 (variable 4) is decreased compared to analysis R2-3 from which it is derived, so the failure index increases. In fact, the maximum failure index for R2-4 exceeds unity, which is a violation of the constraint. The constraint violation problem may possibly be eliminated by changing the value of the DISCOD parameter because this may lead to the selection of different values for the discrete variables. However, the effect of the DISCOD parameter was not investigated further and the default value was used for all of the NASTRN optimization analyses performed in this study. As seen in Table 12, analyses R2-1 and R2-2 yield panel weights that are more than the baseline shown in Table 8, but analyses R2-3 and R2-4 yield panel weights that are significantly less than the baseline weight. All four analyses were stress critical, that is, the stress (failure index) constraint was active and drove the solution. This is also true for analysis R2-2, even though when discrete variables are chosen the failure index does not appear active, because the underlying NASTRAN solution with continuous variables is analysis R2-1 that has an active stress constraint.

Region 3 was optimized using six separate NASTRAN solution 200 analyses. The design variables, type and assigned property IDs for these six analyses are provided in Table 13. Property IDs referenced in the table refer to those defined in Figure 31. The first three analyses (R3-1 – R3-3) correspond to the most easily manufactured panel since the skin face sheet thicknesses and core thickness are uniform throughout the panel. Analyses R3-1 and R3-3 utilize all continuous and all discrete variables, respectively, whereas analysis R3-2 utilizes discrete variables with the exception of the skin core thickness variable, which is continuous. All property sets associated with a particular part of the panel (skin, skin/flange, frame sandwich or frame web) are assigned the same values, which results in a total of six independent design variables and one dependent (calculated) design variable (the frame sandwich core thickness). Analyses R3-4 – R4-6 permit the skin faces and core in the skin/flange property sets to be of different thicknesses than the skin faces and core in the skin only property sets. Analyses R3-4 and R3-6 utilize all continuous and all discrete variables, respectively, while analysis R3-5 utilizes discrete variables with the exception of the skin core thickness variable, which is continuous. Again, similar property sets were assigned the

same values, resulting in a total of nine independent design variables and the dependent frame sandwich core thickness design variable. Results for the six region 3 NASTRAN optimization analyses are presented in Table 14. Analyses R3-1 – R3-3 yield panels with weights slightly larger than the baseline weight shown in Table 8, whereas analyses R3-4 – R3-6 yield panel weights that are slightly less than the baseline weight. All six analyses were buckling critical, and Figure 42 shows the fundamental buckling mode shape for the R3-4 optimization analysis. Mode shapes are similar for the other region 3 analysis cases.

Region 4 was optimized similar to region 3 using six NASTRAN solution 200 analyses. The design variables, type and assigned property IDs for these six analyses are provided in Table 15. Property IDs referenced in Table 15 refer to those defined in Figure 32. The region 4 optimization analyses are defined in a manner identical to those for region 3. Thus, analyses R4-1 – R4-3 have a total of six independent design variables and one dependent design variable, while analyses R4-4 – R4-6 have a total of nine independent design variables and one dependent design variable. Results for the six region 4 NASTRAN optimization analyses are presented in Table 16. All six analyses yield panel weights that are significantly more than the baseline weight shown in Table 8, and were stress (failure index) critical. However, these designs are unrealistic since they appear to be driven by extremely local high stress values at nodes in the frame at the boundary of the panel. Local model modifications were made in an effort to eliminate the high local stresses, but were unsuccessful. Additionally, the stress output requested via the STRESS command was changed from BILIN, which provides output values at the nodes and the centroid, to CENTER, which provides output values only at the centroid, with no effect on the results. This indicates that the output request does not affect the optimization solution. Therefore, it appears that the NASTRAN optimization solution may be susceptible to very high local nodal values, such as those that may arise from singularities and/or modeling, even if these values are unrealistic or spurious. It will be seen in the next section that the GA does not exhibit this behavior since, for the current study, the stresses used in the GA constraint calculation are extracted at the element center and are therefore not unduly influenced by these extreme nodal values.

Table 9: Region 1 NASTRAN optimization analysis design variable assignments

Optimization Analysis	Design Variable #	Designation	Type	Assigned Property IDs
R1-1	1	t_s	Continuous	10 - 45, 50 - 113
	2	t_f	Continuous	50 - 113
	3	t_w	Continuous	120 - 151
R1-2	1	t_s	Discrete	10 - 45, 50 - 113
	2	t_f	Discrete	50 - 113
	3	t_w	Discrete	120 - 151
R1-3	1	t_s	Continuous	10 - 45
	2	t_s	Continuous	50 - 113
	3	t_f	Continuous	50 - 113
	4	t_w	Continuous	120 - 151
R1-4	1	t_s	Discrete	10 - 45
	2	t_s	Discrete	50 - 113
	3	t_f	Discrete	50 - 113
	4	t_w	Discrete	120 - 151

Table 10: Region 1 NASTRAN optimization analysis results

Optimization Analysis	Design Variable #	Value (in.)	Weight (lbs.)	Buckling LF*
R1-1	1	0.72797	164.8	0.354
	2	0.61784		
	3	0.30074		
R1-2	1	0.77 (14 stacks)	173.7	0.397
	2	0.605 (11 stacks)		
	3	0.33 (6 stacks)		
R1-3	1	0.72358	164.3	0.350
	2	1.2932		
	3	0.058511		
	4	0.30232		
R1-4	1	0.77 (14 stacks)	172.4	0.396
	2	1.265 (23 stacks)		
	3	0.055 (1 stack)		
	4	0.33 (6 stacks)		

*Permitted load factors are 0.35 for local buckling and 1.0 for global buckling

Table 11: Region 2 NASTRAN optimization analysis design variable assignments

Optimization Analysis	Design Variable #	Designation	Type	Assigned Property IDs
R2-1	1	t_s	Continuous	10 - 37, 50 - 97
	2	t_f	Continuous	50 - 97
	3	t_w	Continuous	120 - 143
R2-2	1	t_s	Discrete	10 - 37, 50 - 97
	2	t_f	Discrete	50 - 97
	3	t_w	Discrete	120 - 143
R2-3	1	t_s	Continuous	10 - 37
	2	t_s	Continuous	50 - 97
	3	t_f	Continuous	50 - 97
	4	t_w	Continuous	120 - 143
R2-4	1	t_s	Discrete	10 - 37
	2	t_s	Discrete	50 - 97
	3	t_f	Discrete	50 - 97
	4	t_w	Discrete	120 - 143

Table 12: Region 2 NASTRAN optimization analysis results

Optimization Analysis	Design Variable #	Value (in.)	Weight (lbs.)	Failure Index
R2-1	1	0.74753	149.6	0.997
	2	0.055288		
	3	0.13515		
R2-2	1	0.715 (13 stacks)	146.1	0.692
	2	0.11 (2 stacks)		
	3	0.165 (3 stacks)		
R2-3	1	0.36273	83.87	0.999
	2	0.18858		
	3	0.50359		
	4	0.17239		
R2-4	1	0.33 (6 stacks)	79.24	1.10
	2	0.22 (4 stack)		
	3	0.55 (10 stacks)		
	4	0.165 (3 stacks)		

Table 13: Region 3 NASTRAN optimization analysis design variable assignments

Optimization Analysis	Design Variable #	Designation	Type	Assigned Property IDs
R3-1	1	t_{si}	Continuous	10 - 57, 100 - 195
	2	t_c	Continuous	10 - 57, 100 - 195
	3	t_{so}	Continuous	10 - 57, 100 - 195
	4	t_f	Continuous	100 - 195
	5	t_{ss}	Continuous	300 - 339
	6	t_w	Continuous	200 - 239
	7	t_{sc}	Calculated	300 - 339
R3-2	1	t_{si}	Discrete	10 - 57, 100 - 195
	2	t_c	Continuous	10 - 57, 100 - 195
	3	t_{so}	Discrete	10 - 57, 100 - 195
	4	t_f	Discrete	100 - 195
	5	t_{ss}	Discrete	300 - 339
	6	t_w	Discrete	200 - 239
	7	t_{sc}	Calculated	300 - 339
R3-3	1	t_{si}	Discrete	10 - 57, 100 - 195
	2	t_c	Discrete	10 - 57, 100 - 195
	3	t_{so}	Discrete	10 - 57, 100 - 195
	4	t_f	Discrete	100 - 195
	5	t_{ss}	Discrete	300 - 339
	6	t_w	Discrete	200 - 239
	7	t_{sc}	Calculated	300 - 339

Table 13 (cont.): Region 3 NASTRAN optimization analysis design variable assignments

Optimization Analysis	Design Variable #	Designation	Type	Assigned Property IDs
R3-4	1	t_{si}	Continuous	10 - 57
	2	t_c	Continuous	10 - 57
	3	t_{so}	Continuous	10 - 57
	4	t_f	Continuous	100 - 195
	5	t_{si}	Continuous	100 - 195
	6	t_c	Continuous	100 - 195
	7	t_{so}	Continuous	100 - 195
	8	t_{ss}	Continuous	300 - 339
	9	t_w	Continuous	200 - 239
	10	t_{sc}	Calculated	300 - 339
R3-5	1	t_{si}	Discrete	10 - 57
	2	t_c	Continuous	10 - 57
	3	t_{so}	Discrete	10 - 57
	4	t_f	Discrete	100 - 195
	5	t_{si}	Discrete	100 - 195
	6	t_c	Continuous	100 - 195
	7	t_{so}	Discrete	100 - 195
	8	t_{ss}	Discrete	300 - 339
	9	t_w	Discrete	200 - 239
	10	t_{sc}	Calculated	300 - 339
R3-6	1	t_{si}	Discrete	10 - 57
	2	t_c	Discrete	10 - 57
	3	t_{so}	Discrete	10 - 57
	4	t_f	Discrete	100 - 195
	5	t_{si}	Discrete	100 - 195
	6	t_c	Discrete	100 - 195
	7	t_{so}	Discrete	100 - 195
	8	t_{ss}	Discrete	300 - 339
	9	t_w	Discrete	200 - 239
	10	t_{sc}	Calculated	300 - 339

Table 14: Region 3 NASTRAN optimization analysis results

Optimization Analysis	Design Variable #	Value (in.)	Weight (lbs.)	Buckling LF*
R3-1	1	0.055223	319.2	0.982
	2	0.52399		
	3	0.11039		
	4	0.60748		
	5	0.062436		
	6	0.95418		
	7	0.82931		
R3-2	1	0.055 (1 stack)	337.3	0.913
	2	0.52399		
	3	0.11 (2 stacks)		
	4	0.605 (11 stacks)		
	5	0.11 (2 stacks)		
	6	0.99 (18 stacks)		
	7	0.77		
R3-3	1	0.055 (1 stack)	335.0	1.04
	2	0.55		
	3	0.11 (2 stacks)		
	4	0.605 (11 stacks)		
	5	0.11 (2 stack)		
	6	0.935 (17 stacks)		
	7	0.715		

*Permitted load factors are 0.35 for local buckling and 1.0 for global buckling

Table 14 (cont.): Region 3 NASTRAN optimization analysis results

Optimization Analysis	Design Variable #	Value (in.)	Weight (lbs.)	Buckling LF*
R3-4	1	0.056368	276.5	1.00
	2	0.48581		
	3	0.11024		
	4	0.55310		
	5	0.55310		
	6	1.2121		
	7	0.25879		
	8	0.064176		
	9	0.89716		
	10	0.76881		
R3-5	1	0.055 (1 stack)	291.9	1.01
	2	0.48581		
	3	0.11 (2 stacks)		
	4	0.055 (1 stack)		
	5	0.055 (1 stack)		
	6	1.2121		
	7	0.275 (5 stacks)		
	8	0.11 (2 stacks)		
	9	0.88 (16 stacks)		
	10	0.66		
R3-6	1	0.055 (1 stack)	292.5	1.05
	2	0.5		
	3	0.11 (2 stacks)		
	4	0.055 (1 stack)		
	5	0.055 (1 stack)		
	6	1.2		
	7	0.275 (5 stacks)		
	8	0.11 (2 stacks)		
	9	0.88 (16 stacks)		
	10	0.66		

*Permitted load factors are 0.35 for local buckling and 1.0 for global buckling

Table 15: Region 4 NASTRAN optimization analysis design variable assignments

Optimization Analysis	Design Variable #	Designation	Type	Assigned Property IDs
R4-1	1	t_{si}	Continuous	10 - 49, 100 - 179
	2	t_c	Continuous	10 - 49, 100 - 179
	3	t_{so}	Continuous	10 - 49, 100 - 179
	4	t_f	Continuous	100 - 179
	5	t_{ss}	Continuous	300 - 331
	6	t_w	Continuous	200 - 231
	7	t_{sc}	Calculated	300 - 331
R4-2	1	t_{si}	Discrete	10 - 49, 100 - 179
	2	t_c	Continuous	10 - 49, 100 - 179
	3	t_{so}	Discrete	10 - 49, 100 - 179
	4	t_f	Discrete	100 - 179
	5	t_{ss}	Discrete	300 - 331
	6	t_w	Discrete	200 - 231
	7	t_{sc}	Calculated	300 - 331
R4-3	1	t_{si}	Discrete	10 - 49, 100 - 179
	2	t_c	Discrete	10 - 49, 100 - 179
	3	t_{so}	Discrete	10 - 49, 100 - 179
	4	t_f	Discrete	100 - 179
	5	t_{ss}	Discrete	300 - 331
	6	t_w	Discrete	200 - 231
	7	t_{sc}	Calculated	300 - 331

Table 15 (cont.): Region 4 NASTRAN optimization analysis design variable assignments

Optimization Analysis	Design Variable #	Designation	Type	Assigned Property IDs
R4-4	1	t_{si}	Continuous	10 - 49
	2	t_c	Continuous	10 – 49
	3	t_{so}	Continuous	10 - 49
	4	t_f	Continuous	100 - 179
	5	t_{si}	Continuous	100 - 179
	6	t_c	Continuous	100 - 179
	7	t_{so}	Continuous	100 - 179
	8	t_{ss}	Continuous	300 - 331
	9	t_w	Continuous	200 - 231
	10	t_{sc}	Calculated	300 - 331
R4-5	1	t_{si}	Discrete	10 - 49
	2	t_c	Continuous	10 – 49
	3	t_{so}	Discrete	10 - 49
	4	t_f	Discrete	100 - 179
	5	t_{si}	Discrete	100 - 179
	6	t_c	Continuous	100 - 179
	7	t_{so}	Discrete	100 - 179
	8	t_{ss}	Discrete	300 - 331
	9	t_w	Discrete	200 - 231
	10	t_{sc}	Calculated	300 - 331
R4-6	1	t_{si}	Discrete	10 - 49
	2	t_c	Discrete	10 – 49
	3	t_{so}	Discrete	10 - 49
	4	t_f	Discrete	100 - 179
	5	t_{si}	Discrete	100 - 179
	6	t_c	Discrete	100 - 179
	7	t_{so}	Discrete	100 - 179
	8	t_{ss}	Discrete	300 - 331
	9	t_w	Discrete	200 - 231
	10	t_{sc}	Calculated	300 - 331

Table 16: Region 4 NASTRAN optimization analysis results

Optimization Analysis	Design Variable #	Value (in.)	Weight (lbs.)	Failure Index
R4-1	1	0.43089	950.1	0.986
	2	0.081016		
	3	0.25464		
	4	1.10000		
	5	0.10650		
	6	1.1716		
	7	0.95860		
R4-2	1	0.385 (7 stacks)	865.0	1.05
	2	0.081016		
	3	0.22 (4 stacks)		
	4	1.045 (19 stacks)		
	5	0.11 (2 stacks)		
	6	1.155 (21 stacks)		
	7	0.935		
R4-3	1	0.385 (7 stacks)	863.1	0.928
	2	0.05		
	3	0.22 (4 stacks)		
	4	1.045 (19 stacks)		
	5	0.11 (2 stacks)		
	6	1.155 (21 stacks)		
	7	0.935		

Table 16 (cont.): Region 4 NASTRAN optimization analysis results

Optimization Analysis	Design Variable #	Value (in.)	Weight (lbs.)	Failure Index
R4-4	1	0.22795	916.9	1.05
	2	0.05000		
	3	0.43170		
	4	1.0992		
	5	0.066349		
	6	0.05000		
	7	0.16611		
	8	0.11000		
	9	1.7739		
	10	1.5539		
R4-5	1	0.275 (5 stacks)	954.0	1.06
	2	0.05000		
	3	0.44 (8 stacks)		
	4	1.045 (19 stacks)		
	5	0.055 (1 stack)		
	6	0.05000		
	7	0.165 (3 stacks)		
	8	0.11 (2 stacks)		
	9	1.815 (33 stacks)		
	10	1.595		
R4-6	1	0.275 (5 stacks)	954.0	1.06
	2	0.05000		
	3	0.44 (8 stacks)		
	4	1.045 (19 stacks)		
	5	0.055 (1 stack)		
	6	0.05000		
	7	0.165 (3 stacks)		
	8	0.11 (2 stacks)		
	9	1.815 (33 stacks)		
	10	1.595		

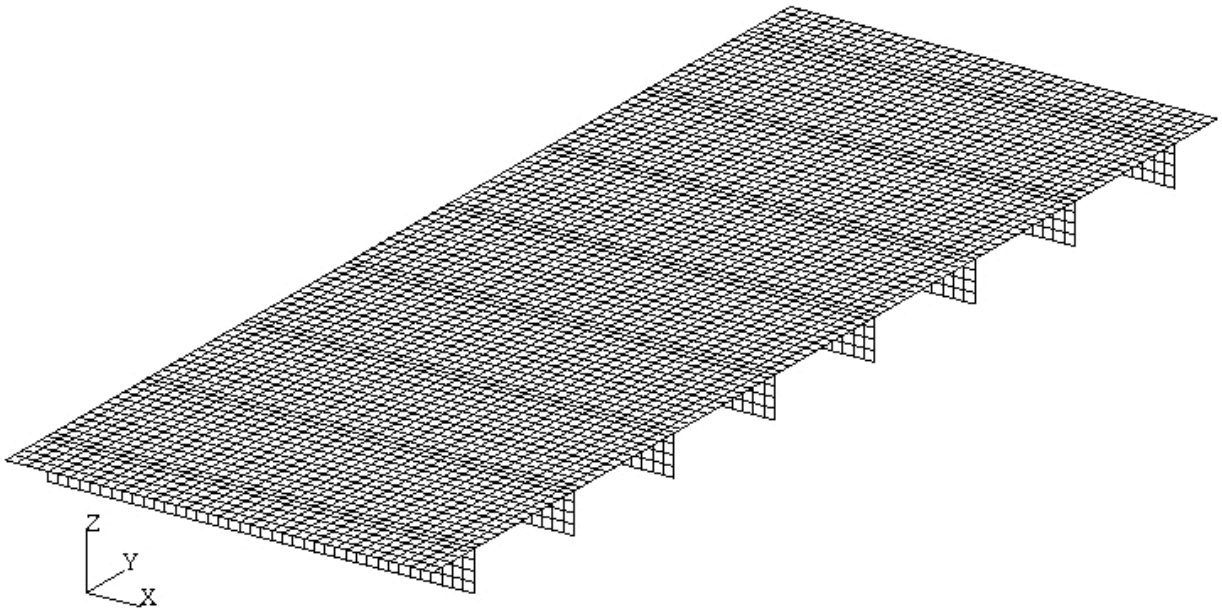

Figure 33: Finite element mesh for region 1

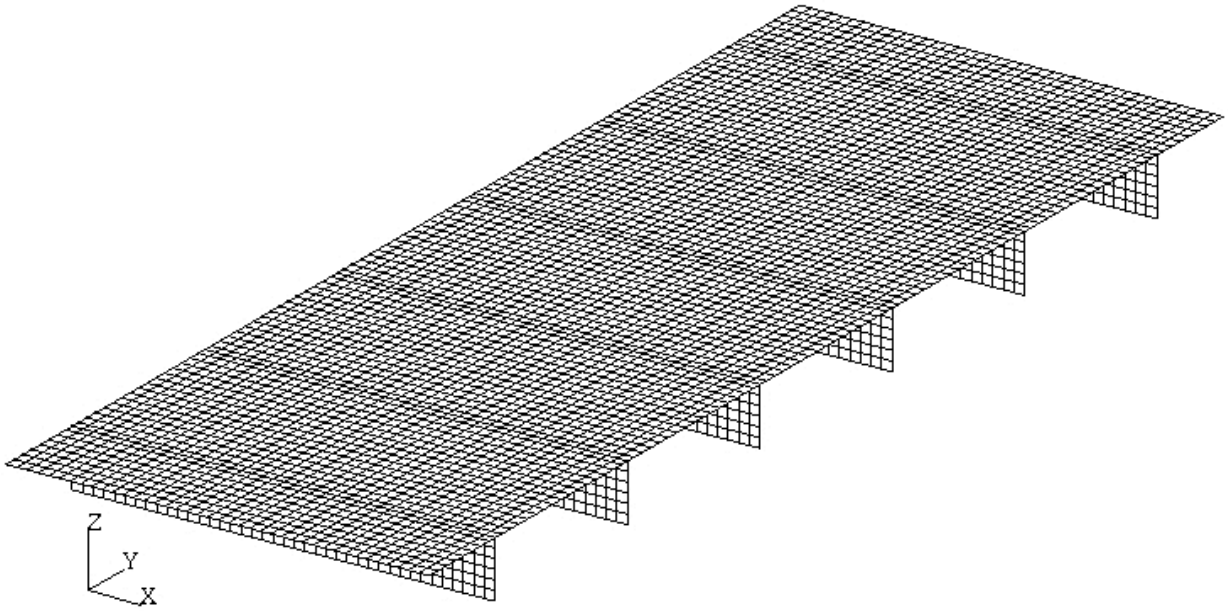

Figure 34: Finite element mesh for region 2

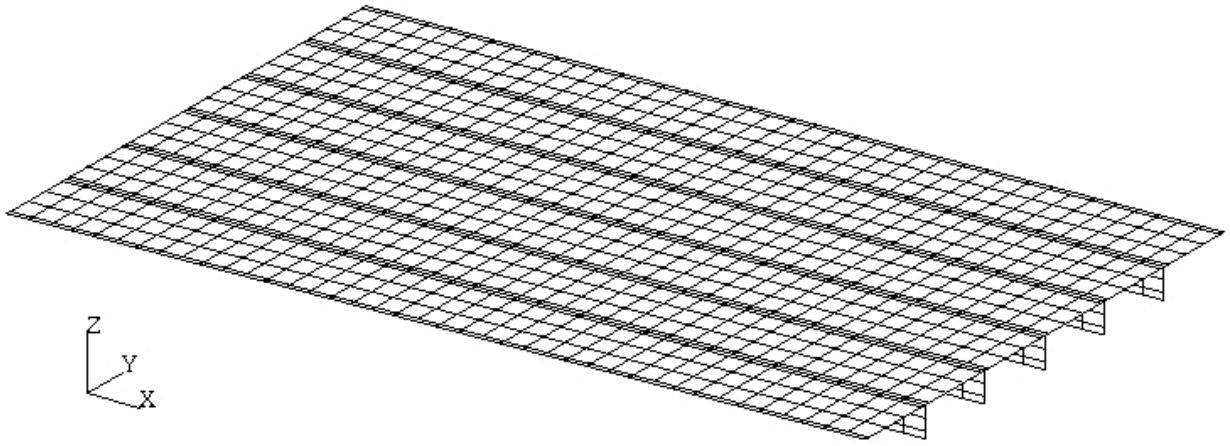

Figure 35: Finite element mesh for region 3

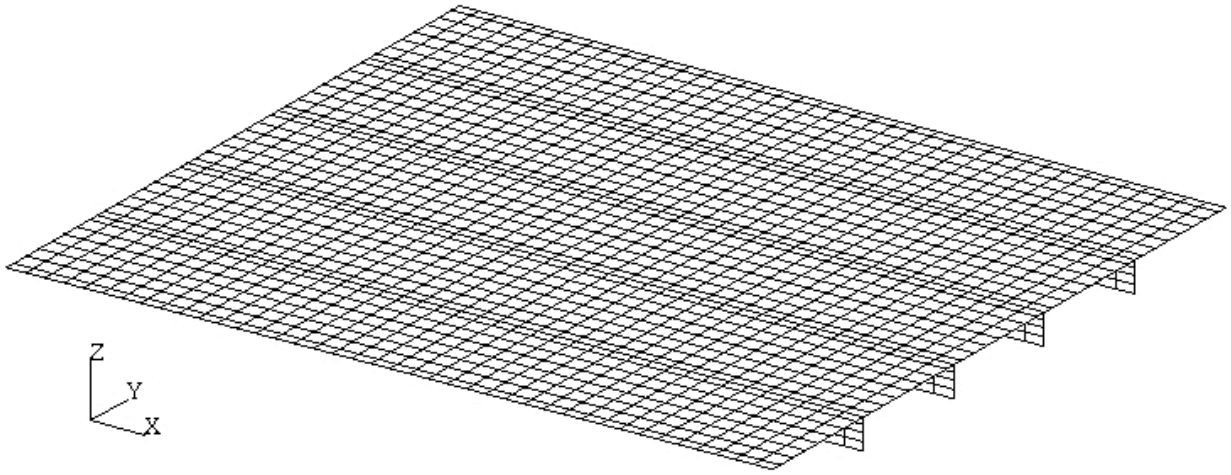

Figure 36: Finite element mesh for region 4

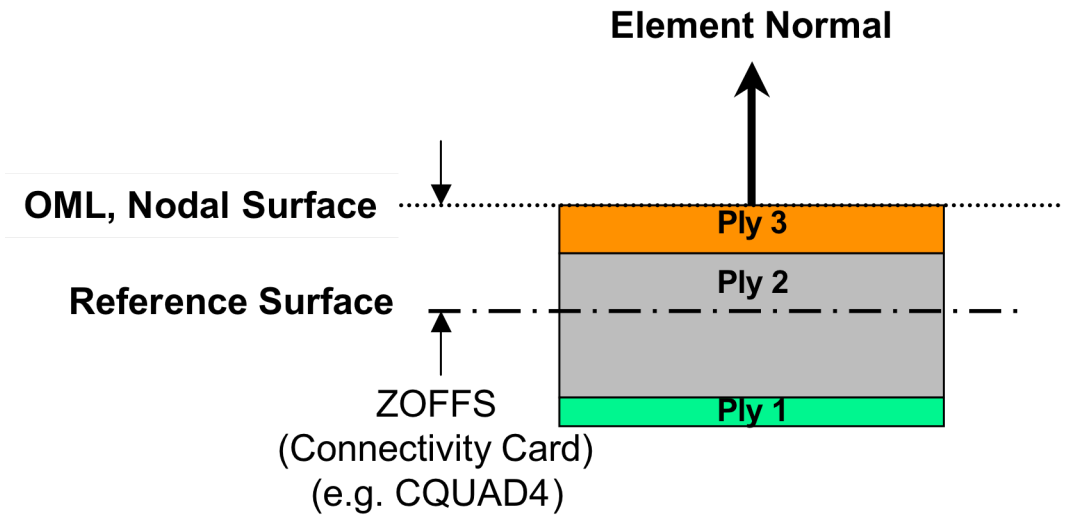

a) Original (ZOFFS = -t/2)

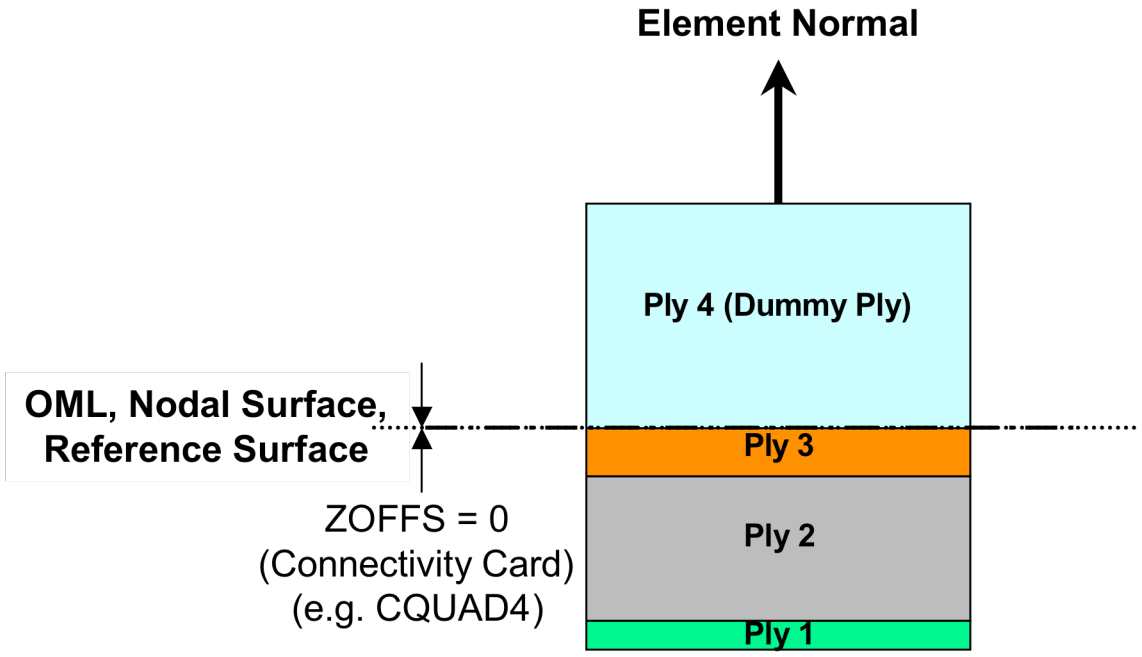

b) Dummy Ply (ZOFFS = 0)

Figure 37: Dummy ply used to eliminate offset (ZOFFS)

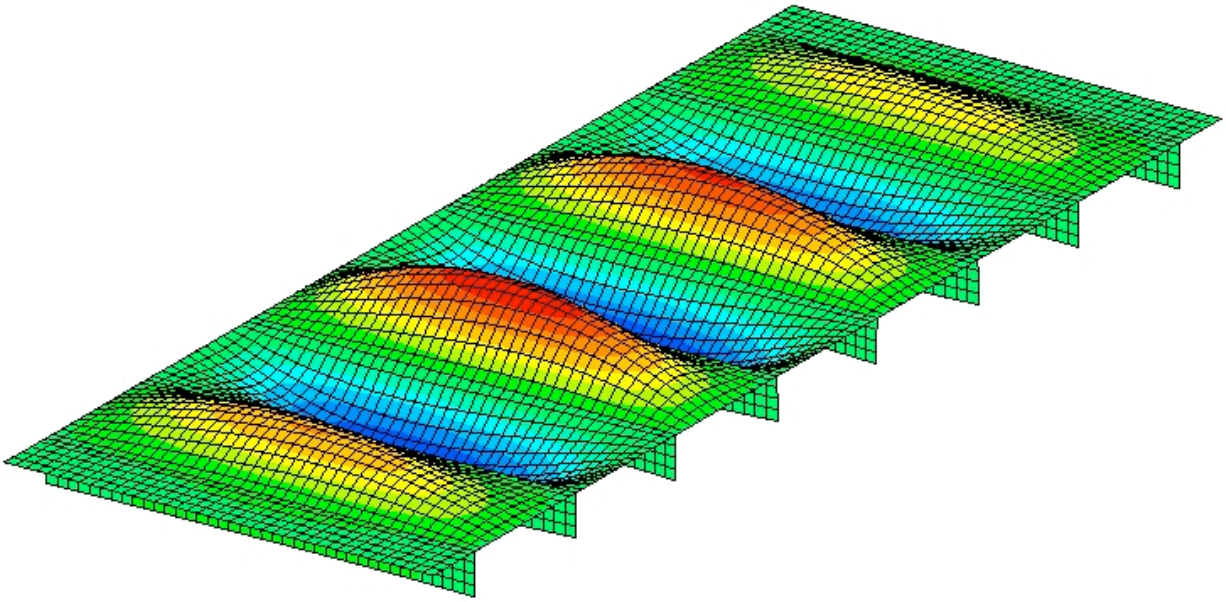

Figure 38: Original fundamental buckling mode shape for region 1, λ = 0.131

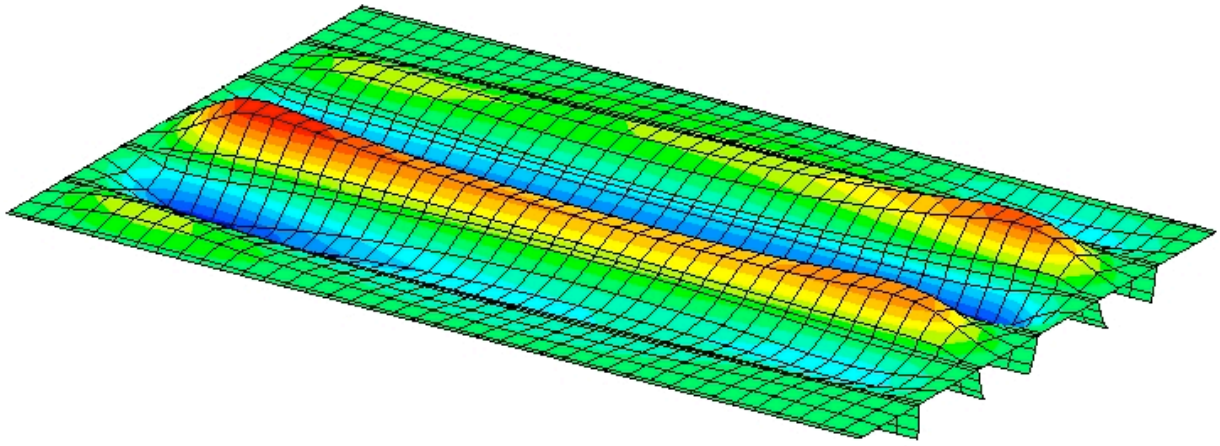

Figure 39: Original fundamental buckling mode shape for region 3, λ = 0.623

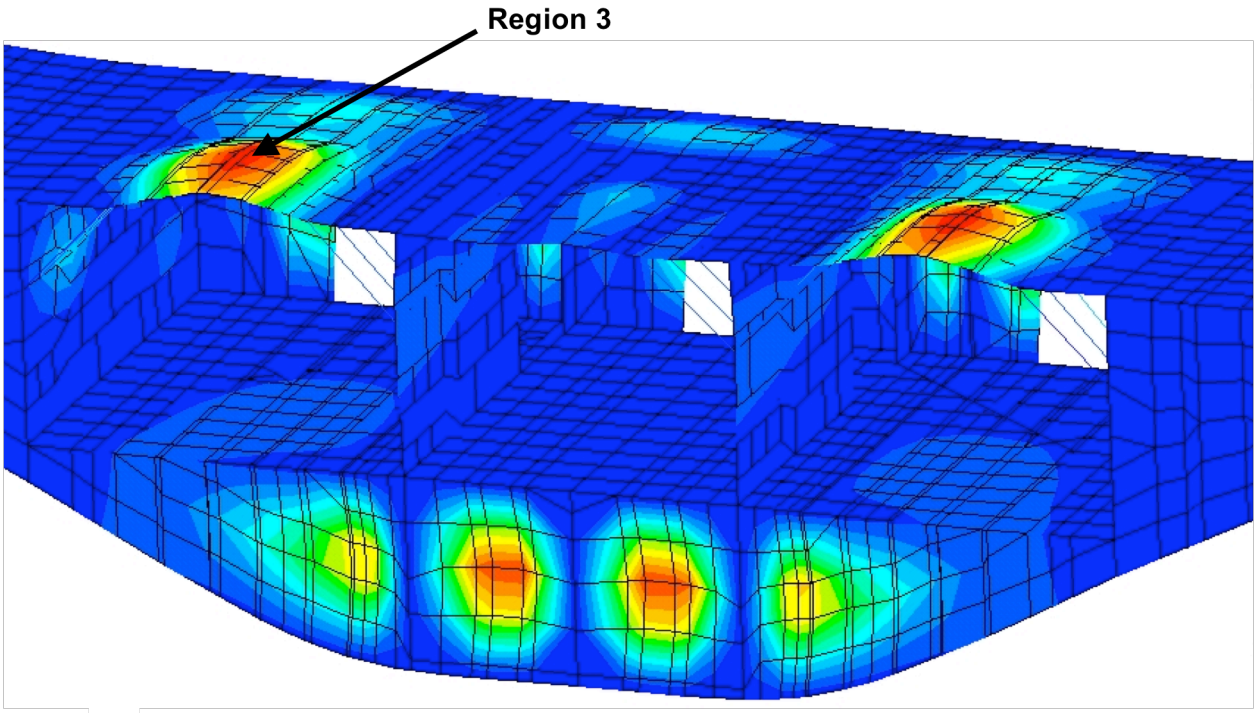

Figure 40: Nonlinear global deformations in the vicinity of region 3

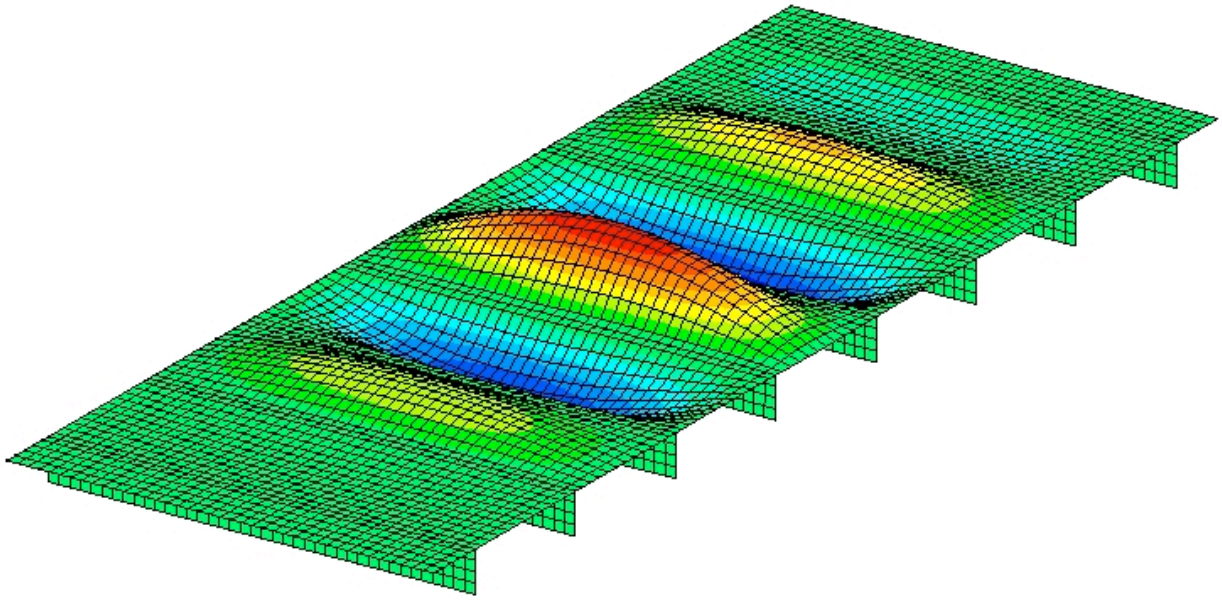

Figure 41: Optimized fundamental buckling mode shape for region 1, λ = 0.350

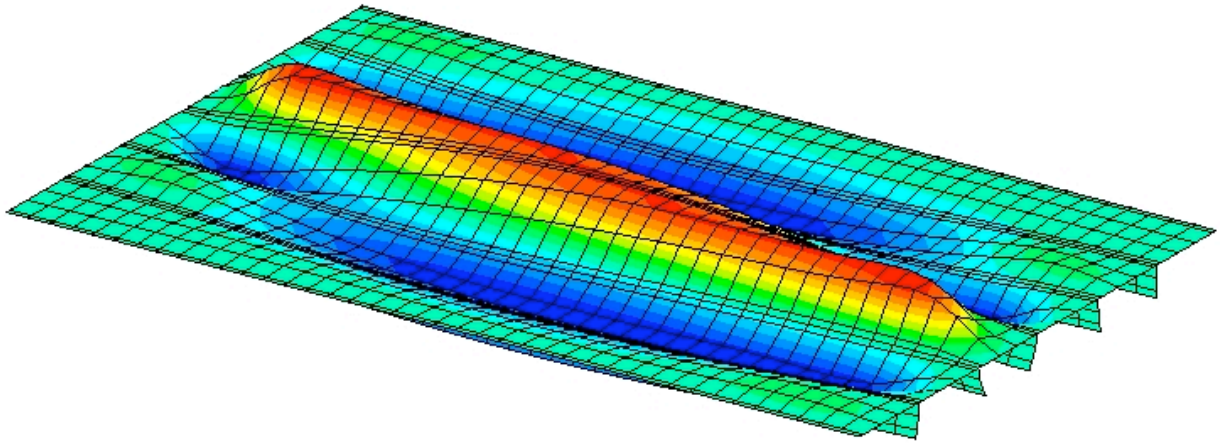

Figure 42: Optimized fundamental buckling mode shape for region 3, λ = 1.00

Genetic Algorithm

Many optimization techniques are available, including a class referred to as probabilistic search algorithms. Probabilistic search algorithms, such as genetic algorithm (GA) and simulated annealing, are types of probabilistic searches that are well suited to problems potentially having many local optima. Analyses using discrete design variables are particularly prone to having many local optima, therefore, the GA is a prime choice for finding the global optimum in the current study. Genetic algorithms are credited to Holland [12] and were made popular by Goldberg [13]. References 14 – 16 pertain to genetic algorithms, and readers are encouraged to consult these and other references for details of the GA. A brief synopsis of the genetic algorithm as implemented for this study is included herein.

GAs make use of genetic operators, such as reproduction, cross-over, mutation and permutation. These operators are applied to individual designs, termed chromosomes, whose components (genes) are representations of the design variables. An initial set of designs is generated randomly and is termed the initial population. Each design in the initial population is evaluated and is assigned a "fitness" based upon the objective function and constraints, and the population is ranked based by these fitnesses. Two "parents" are randomly chosen for reproduction based on their fitnesses, with designs having an increased probability of being picked with improving fitness. From the parent designs, "children" designs are created by means of cross-over. Cross-over is an operation through which parts of the parent designs are chosen and then combined to create a new design. These children can then be subjected to mutation (random change in a gene value), permutation (re-arranging of certain genes) and other operators in order to create designs that would otherwise not be possible through cross-over, alone. The child population is again ranked based upon fitness, and the process continues until the best fitness does not improve in successive populations (i.e., the improvement in fitness is within a specified threshold). The optimum design is the design that is associated with this converged, best fitness.

An author-written, FORTRAN code was used in the current study. This GA code utilized NASTRAN to perform finite element analyses of each design and extracts response data to formulate the fitness function. The fitness function was defined as:

$$Fitness = w_w * weight\_ratio + w_s * stress\_constr + w_b * buckling\_constr$$

where the w_i's are the weight multipliers assigned to the panel total weight ratio (*weight_ratio*), stress constraint (*stress_constr*) and buckling constraint (*buckling_constr*). The total weight ratio is the structural weight calculated by NASTRAN divided by the weight of the baseline design (in this case the associated Boeing design). The stress and buckling constraints were defined as follows:

$$stress\_constr = \begin{cases} FI - 1 & , \ FI > 1 \\ 0 & , \ FI \le 1 \end{cases}$$

$$buckling\_constr = \begin{cases} \lambda_{allow} - \lambda_1 & , \ \lambda_{allow} > \lambda_1 \\ 0 & , \ \lambda_{allow} \le \lambda_1 \end{cases}$$

where FI is the Tsai-Hill failure index previously defined, λ_{allow} is the allowable buckling load factor, and λ_1 is the fundamental buckling load factor for the design. Constraints for the GA are evaluated at the element centroid, and therefore avoid problems that may arise due to large local nodal values, as was observed in the NASTRAN optimization analyses for region 4.

In this study, the genes in the chromosomes represent the number of stacks assigned to a design variable that defines a particular ply thickness in a shell property PCOMP entry definition. Minimum and maximum stack (thickness) values are enforced directly in the code when designs are being created (i.e., the assigned gene value can not be outside the prescribed limits). Minimum values assigned to the design variables are the same as those used in the NASTRAN solution 200 analyses and shown in Table 7, but for the genetic algorithm no maximum values were imposed. Therefore, the GA as implemented treats all design variables as discrete, with the core thickness increment being the aforementioned 0.05 inches.

The author-written GA code utilizes three types of cross-over, namely single-point, double-point and uniform-point cross-over. The code also utilizes mutation and permutation. However, permutation does not work well for these panels because there is a large discrepancy in the number of stacks assigned to the variables. Permutation in such cases can lead to buckling performance problems for the design that lead to NASTRAN errors, and result in an unsuccessful analysis due to premature termination of the GA code. The reliable inclusion of permutation requires modification to the current code. Therefore, since such modifications have not yet been made, permutation was omitted from this current study.

The finite element models used as the baseline for each region are the same as those previously shown for the NASTRAN optimization in Figures 33 – 36. During optimization, the GA code modifies the property definitions in the baseline NASTRAN files in accordance with the design chromosomes. The initial GA analyses were limited to the cases examined using discrete design variables in the NASTRAN optimization. GA optimization analysis specifications and their results are provided in Tables 17 – 20 for the four trade study regions. Compared to the baselines, region 1 shows a weight increase and regions 2 – 4 show a weight reduction.

In a manner similar to the NASTRAN optimization analyses, increasing the number of design variables in the GA optimization generally resulted in poor convergence and unrealistic results. However, region 4 was examined further by increasing the number of design variables by creating bands of similar properties along the panel edges. Figure 43 shows the color-coded property bands for the two additional analysis definitions provided in Tables 21 and 22. Results for these additional analyses are given in Table 23. It is seen that these additional analyses result in much lower weight panels than the uniform panels previously optimized. This is a result of the double bending curvature experienced by the pressurized panel (center and edges of the panel bending in opposite directions), a phenomenon also observed and discussed in Reference 6. This result emphasizes the potential inefficiency of a uniform panel design and suggests that panel tailoring will lead to more optimum designs.

Table 17: Region 1 GA optimization analysis results

Optimization Analysis	Design Variable #	Value (in.)	Weight (lbs.)	Buckling LF*
R1-2	1	0.77 (14 stacks)	162.1	0.366
	2	0.11 (2 stacks)		
	3	0.33 (6 stacks)		
R1-4	1	0.77 (14 stacks)	166.7	0.350
	2	0.605 (11 stacks)		
	3	0.11 (2 stacks)		
	4	0.495 (9 stacks)		

*Permitted load factors are 0.35 for local buckling and 1.0 for global buckling

Table 18: Region 2 GA optimization analysis results

Optimization Analysis	Design Variable #	Value (in.)	Weight (lbs.)	Failure Index
R2-2	1	0.275 (5 stacks)	73.01	0.900
	2	0.22 (4 stacks)		
	3	0.385 (7 stacks)		
R2-4	1	0.275 (5 stacks)	72.88	0.859
	2	0.44 (8 stacks)		
	3	0.33 (6 stacks)		
	4	0.22 (4 stacks)		

Table 19: Region 3 GA optimization analysis results

Optimization Analysis	Design Variable #	Value (in.)	Weight (lbs.)	Buckling LF*
R3-3	1	0.055 (1 stack)	276.7	1.04
	2	0.55		
	3	0.11 (2 stacks)		
	4	0.055 (1 stack)		
	5	0.11 (2 stacks)		
	6	0.935 (17 stacks)		
	7	0.715		
R3-6	1	0.055 (1 stack)	274.6	1.00
	2	0.5		
	3	0.11 (2 stacks)		
	4	0.055 (1 stack)		
	5	0.055 (1 stack)		
	6	0.6		
	7	0.11 (2 stacks)		
	8	0.11 (2 stacks)		
	9	0.935 (17 stacks)		
	10	0.715		

*Permitted load factors are 0.35 for local buckling and 1.0 for global buckling

Table 20: Region 4 GA optimization analysis results

Optimization Analysis	Design Variable #	Value (in.)	Weight (lbs.)	Failure Index
R4-3	1	0.055 (1 stack)	351.3	0.940
	2	0.2		
	3	0.11 (2 stacks)		
	4	0.11 (2 stacks)		
	5	0.33 (6 stacks)		
	6	1.21 (22 stacks)		
	7	0.55		
R4-6	1	0.055 (1 stack)	351.3	0.940
	2	0.2		
	3	0.11 (2 stacks)		
	4	0.11 (2 stacks)		
	5	0.055 (1 stack)		
	6	0.2		
	7	0.11 (2 stacks)		
	8	0.33 (6 stacks)		
	9	1.21 (22 stacks)		
	10	0.55		

Table 21: Region 4 optimization analysis R4-7 design variable assignments

Design Variable #	Designation	Type	Assigned Property IDs
1	t_{si}	Discrete	11 - 16, 19 - 24, 27 - 32, 35 - 40, 43 - 48, 101 - 106, 109 - 114, 117 - 122, 125 - 130, 133 - 138, 141 - 146, 149 - 154, 157 - 162, 165 - 170, 173 - 178
2	t_c	Discrete	11 - 16, 19 - 24, 27 - 32, 35 - 40, 43 - 48, 101 - 106, 109 - 114, 117 - 122, 125 - 130, 133 - 138, 141 - 146, 149 - 154, 157 - 162, 165 - 170, 173 - 178
3	t_{so}	Discrete	11 - 16, 19 - 24, 27 - 32, 35 - 40, 43 - 48, 101 - 106, 109 - 114, 117 - 122, 125 - 130, 133 - 138, 141 - 146, 149 - 154, 157 - 162, 165 - 170, 173 - 178
4	t_f	Discrete	101 - 106, 109 - 114, 117 - 122, 125 - 130, 133 - 138, 141 - 146, 149 - 154, 157 - 162, 165 - 170, 173 - 178
5	t_{ss}	Discrete	301 - 306, 309 - 314, 317 - 322, 325 - 330
6	t_w	Discrete	201 - 206, 209 - 214, 217 - 222, 225 - 230
7	t_{sc}	Calculated	301 - 306, 309 - 314, 317 - 322, 325 - 330
8	t_{si}	Discrete	10, 17, 18, 25, 26, 33, 34, 41, 42, 49, 100, 107, 108, 115, 116, 123, 124, 131, 132, 139, 140, 147, 148, 155, 156, 163, 164, 171, 172, 179
9	t_c	Discrete	10, 17, 18, 25, 26, 33, 34, 41, 42, 49, 100, 107, 108, 115, 116, 123, 124, 131, 132, 139, 140, 147, 148, 155, 156, 163, 164, 171, 172, 179
10	t_{so}	Discrete	10, 17, 18, 25, 26, 33, 34, 41, 42, 49, 100, 107, 108, 115, 116, 123, 124, 131, 132, 139, 140, 147, 148, 155, 156, 163, 164, 171, 172, 179
11	t_f	Discrete	100, 107, 108, 115, 116, 123, 124, 131, 132, 139, 140, 147, 148, 155, 156, 163, 164, 171, 172, 179
12	t_{ss}	Discrete	300, 307, 308, 315, 316, 323, 324, 331
13	t_w	Discrete	200, 207, 208, 215, 216, 223, 224, 231
14	t_{sc}	Calculated	300, 307, 308, 315, 316, 323, 324, 331

Table 22: Region 4 optimization analysis R4-8 design variable assignments

Design Variable #	Designation	Type	Assigned Property IDs
1	t_{si}	Discrete	12 - 15, 20 - 23, 28 - 31, 36 - 39, 44 - 47, 102 - 105, 110 - 113, 118 - 121, 126 - 129, 134 - 137, 142 - 145, 150 - 153, 158 - 161, 166 - 169, 174 - 177
2	t_c	Discrete	12 - 15, 20 - 23, 28 - 31, 36 - 39, 44 - 47, 102 - 105, 110 - 113, 118 - 121, 126 - 129, 134 - 137, 142 - 145, 150 - 153, 158 - 161, 166 - 169, 174 - 177
3	t_{so}	Discrete	12 - 15, 20 - 23, 28 - 31, 36 - 39, 44 - 47, 102 - 105, 110 - 113, 118 - 121, 126 - 129, 134 - 137, 142 - 145, 150 - 153, 158 - 161, 166 - 169, 174 - 177
4	t_f	Discrete	102 - 105, 110 - 113, 118 - 121, 126 - 129, 134 - 137, 142 - 145, 150 - 153, 158 - 161, 166 - 169, 174 - 177
5	t_{ss}	Discrete	302 - 305, 310 - 313, 318 - 321, 326 - 329
6	t_w	Discrete	202 - 205, 210 - 213, 218 - 221, 226 - 229
7	t_{sc}	Calculated	302 - 305, 310 - 313, 318 - 321, 326 - 329
8	t_{si}	Discrete	10, 17, 18, 25, 26, 33, 34, 41, 42, 49, 100, 107, 108, 115, 116, 123, 124, 131, 132, 139, 140, 147, 148, 155, 156, 163, 164, 171, 172, 179
9	t_c	Discrete	10, 17, 18, 25, 26, 33, 34, 41, 42, 49, 100, 107, 108, 115, 116, 123, 124, 131, 132, 139, 140, 147, 148, 155, 156, 163, 164, 171, 172, 179
10	t_{so}	Discrete	10, 17, 18, 25, 26, 33, 34, 41, 42, 49, 100, 107, 108, 115, 116, 123, 124, 131, 132, 139, 140, 147, 148, 155, 156, 163, 164, 171, 172, 179
11	t_f	Discrete	100, 107, 108, 115, 116, 123, 124, 131, 132, 139, 140, 147, 148, 155, 156, 163, 164, 171, 172, 179
12	t_{ss}	Discrete	300, 307, 308, 315, 316, 323, 324, 331
13	t_w	Discrete	200, 207, 208, 215, 216, 223, 224, 231
14	t_{sc}	Calculated	300, 307, 308, 315, 316, 323, 324, 331
15	t_{si}	Discrete	11, 16, 19, 24, 27, 32, 35, 40, 43, 48, 101, 106, 109, 114, 117, 122, 125, 130, 133, 138, 141, 146, 149, 154, 157, 162, 165, 170, 173, 178
16	t_c	Discrete	11, 16, 19, 24, 27, 32, 35, 40, 43, 48, 101, 106, 109, 114, 117, 122, 125, 130, 133, 138, 141, 146, 149, 154, 157, 162, 165, 170, 173, 178
17	t_{so}	Discrete	11, 16, 19, 24, 27, 32, 35, 40, 43, 48, 101, 106, 109, 114, 117, 122, 125, 130, 133, 138, 141, 146, 149, 154, 157, 162, 165, 170, 173, 178
18	t_f	Discrete	101, 106, 109, 114, 117, 122, 125, 130, 133, 138, 141, 146, 149, 154, 157, 162, 165, 170, 173, 178
19	t_{ss}	Discrete	301, 306, 309, 314, 317, 322, 325, 330
20	t_w	Discrete	201, 206, 209, 214, 217, 222, 225, 230
21	t_{sc}	Calculated	301, 306, 309, 314, 317, 322, 325, 330

Table 23: Additional Region 4 GA optimization analysis results

Optimization Analysis	Design Variable #	Value (in.)	Weight (lbs.)	Failure Index
R4-7	1	0.055 (1 stack)	259.5	0.997
	2	0.1		
	3	0.11 (2 stacks)		
	4	0.055 (1 stack)		
	5	0.11 (2 stacks)		
	6	0.385 (7 stacks)		
	7	0.165		
	8	0.055 (1 stack)		
	9	0.25		
	10	0.11 (2 stacks)		
	11	0.165 (3 stacks)		
	12	0.33 (6 stacks)		
	13	1.265 (23 stacks)		
	14	0.605		
R4-8	1	0.055 (1 stack)	250.9	0.951
	2	0.1		
	3	0.11 (2 stacks)		
	4	0.055 (1 stack)		
	5	0.055 (1 stacks)		
	6	0.385 (7 stacks)		
	7	0.275		
	8	0.055 (1 stack)		
	9	0.1		
	10	0.11 (2 stacks)		
	11	0.33 (6 stack)		
	12	0.275 (5 stacks)		
	13	1.1 (20 stacks)		
	14	0.55		
	15	0.055 (1 stack)		
	16	0.1		
	17	0.11 (2 stacks)		
	18	0.055 (1 stack)		
	19	0.11 (2 stacks)		
	20	0.275 (5 stacks)		
	21	0.055		

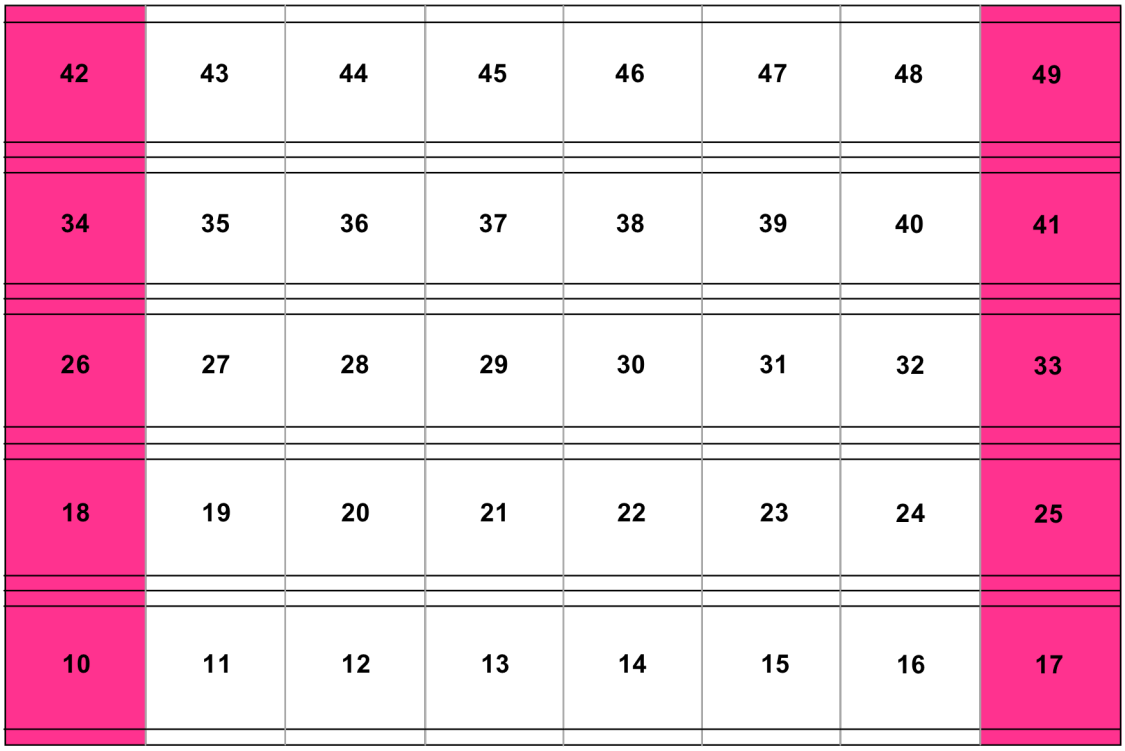

a) Analysis R4-7

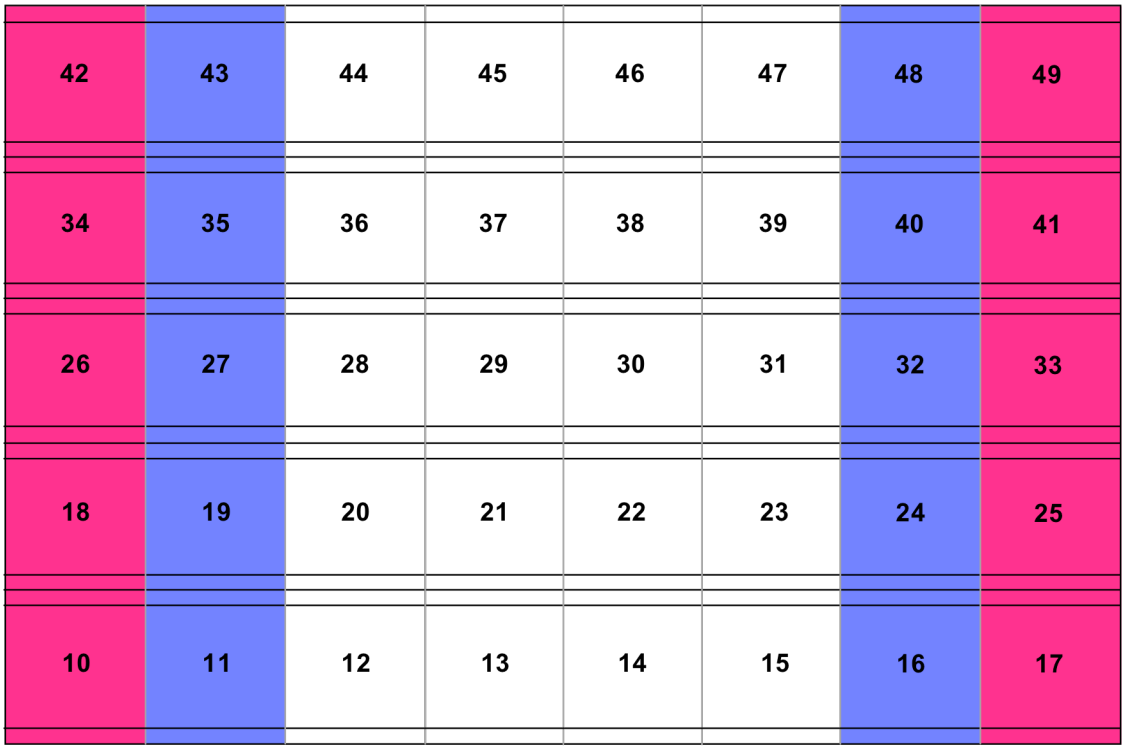

b) Analysis R4-8

Figure 43: Property bands for additional Panel #4 optimization analyses (skin property IDs shown for clarity)

Discussion of Results and Comparison of Methods

The previous two sections presented the optimization analysis methods and the results obtained for the four trade study regions using the NASTRAN solution 200 and GA, respectively. This section provides a discussion of these results and a comparison of the two methods. Recall, however, that only one load case was utilized for each region in this optimization study. Use of other, or additional, load cases may produce markedly different results.

Table 24 summarizes the optimized weights for the trade study regions using the applied optimization methods. In general, for all regions the GA analysis produced panel weights similar to or less than the weights from the NASTRAN analyses. Also, recall that the NASTRAN optimization analysis results for region 4 are unrealistic due to being driven by large local nodal stress values. This study found that region 1 showed a small weight increase over the baseline design, region 2 showed significant decrease in weight over the baseline design, region 3 showed a small decrease in weight over the baseline although the NASTRAN results were split, and region 4 showed a significant decrease in weight over the baseline when a larger number of design variables was used.

For several of the NASTRAN optimization analyses the constraints are not satisfied (e.g., buckling load factor for analysis R1-2 and the failure index for analysis R2-4), whereas the genetic algorithm was forced to satisfy constraints, and thus always yielded feasible solutions. Some of the optimization analyses were designed to ensure that the optimized configuration retained the same general baseline skin/stiffener configurations shown in Figures 26 and 27, with only the thicknesses being varied. However, several other optimization analyses did permit configurations that varied slightly from the baseline. For example, in regions 1 and 2, it is possible that the optimized solution results in the configurations shown in Figures 44 and 45. It is obvious that multiple optima having the same weight can exist for regions 1 and 2 because the thicknesses can be adjusted so that the total skin/flange thickness can be obtained by various skin and flange thickness combinations. Figure 46 shows a possible configuration for the sandwich skin regions. For these sandwich skin construction regions, regions 3 and 4, same weight multiple optima can occur when the inner skin/flange total thickness exceeds the sum of the minimum thicknesses for the inner skin and flange and the thickness of the remaining inner skin. So, in general, the solutions provided herein for all regions are may not necessarily be unique.

Lastly, consider how the optimizations would affect the overall weight of the BWB design. The baseline total weight of the four panels studied was approximately 926 lbs., whereas the optimized total weight was approximately 760 lbs. when using the minimum weights provided by the GA analyses. This is a 17.9% weight reduction. This weight reduction is specific to a very limited set of load cases (2.5G maneuver, 2.5G maneuver with internal pressure, and 2P overpressure) with a single load case being applied to each panel optimization. Increasing the number of included load cases, and/or increasing the applied load cases, may result in significantly different optimization results.

Table 24: Optimization analysis panel weight results

		Weight (lbs.)		
Region #	Optimization Analysis	Original Baseline	NASTRAN Solution 200	Genetic Algorithm
1	R1-1	153.5	164.8	NA
	R1-2		173.7	162.1
	R1-3		164.3	NA
	R1-4		172.4	166.7
2	R2-1	120.1	149.6	NA
	R2-2		146.1	73.01
	R2-3		83.87	NA
	R2-4		79.24	72.88
3	R3-1	299.7	319.2	NA
	R3-2		337.3	NA
	R3-3		335.0	276.7
	R3-4		276.5	NA
	R3-5		291.9	NA
	R3-6		292.5	274.6
4	R4-1	362.5	950.1	NA
	R4-2		865.0	NA
	R4-3		863.1	351.3
	R4-4		916.9	NA
	R4-5		954.0	NA
	R4-6		954.0	351.3
	R4-7		NA	259.5
	R4-8		NA	250.9

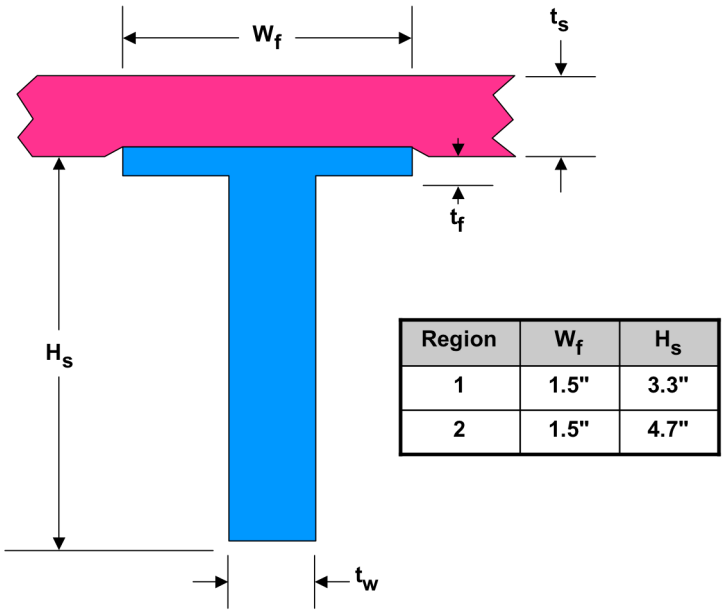

Figure 44: Region 1 and 2 configuration where skin under the flange is thinner than the surrounding skin thickness

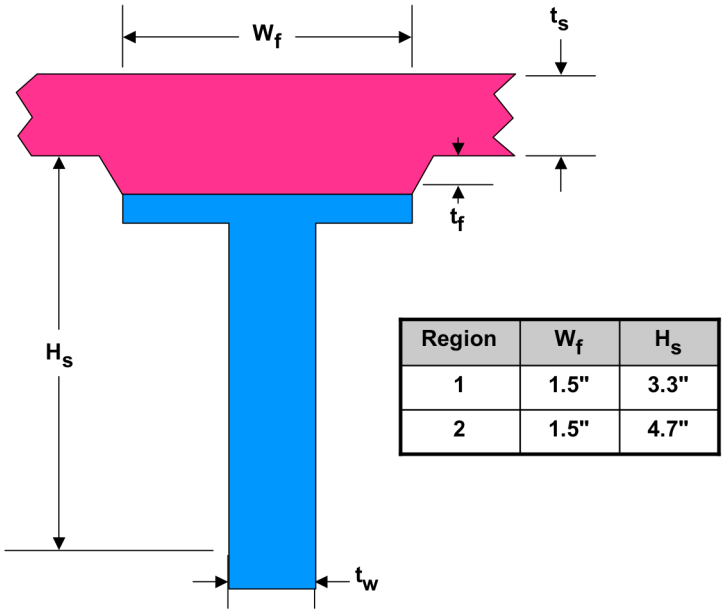

Region	W_f	H_s
1	1.5"	3.3"
2	1.5"	4.7"

Figure 45: Region 1 and 2 configuration where skin under the flange is thicker than the surrounding skin thickness

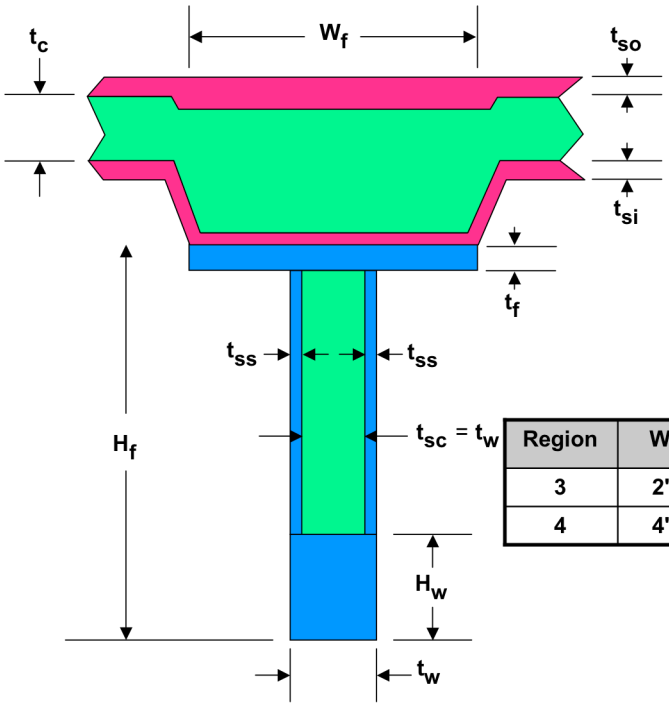

Region	W_f	H_f	H_w
3	2"	5.5"	1.25"
4	4"	5.5"	3"

Figure 46: Regions 3 and 4 configuration where the sandwich skin under the flange has thicknesses differing from the surrounding skin

Summary/Conclusion

Panels from four regions of a representative 3-bay, 400,000 lb. GTW BWB design were optimized using NASTRAN solution 200 and genetic algorithm. Each panel region was optimized for a most critical load case that was chosen from a limited set of load cases. The boundary tractions applied to the panels during the optimization analyses were obtained from nonlinear analyses of a full BWB global model. Design concepts for the optimized panels are the same as their corresponding baseline designs, so that the optimization designs are basically a resizing of the baseline designs. However, simplifications were made to the panels in order to facilitate easier modeling and analysis. Simplifications included considering the panels to be flat (ignoring the large radii of curvature), and having uniform edge loads and idealized boundary conditions.

The optimization analyses indicated an approximate total weight savings of nearly 18% for the regions considered in this study. However, this weight savings cannot be extrapolated to the entire BWB design because the regions studied are an extremely small portion of the overall BWB design. In order to get a better weight reduction estimate, more regions should be studied and the simplifications that have been made should be relaxed. Also, the optimization analyses should incorporate significantly more design variables so that the panels can have more tailored designs. Tailoring of the panels can be of particular interest for panels not having uniform loading and/or idealized boundary conditions. Optimization studies should also be carried out on other panel construction types to determine if other structural concepts will yield lighter designs (this study considered only panels of the same type of construction as the baseline BWB designs). This preliminary optimization analysis indicates that improvements can be made to the baseline BWB design, but more work needs to be done to determine exactly how much improvement can be made, and how this improvement will be realized.

References

[1]Liebeck, R., "Design of the Blended-Wing-Body Subsonic Transport", Paper AIAA-2002-0002, 40th AIAA Aerospace Sciences Meeting & Exhibit, Reno, Nevada, January 14-17, 2002.

[2]Liebeck, R., "Design of the Blended Wing Body Subsonic Transport", *Journal of Aircraft*, Vol. 41, No. 1, January-February, 2004, pp. 10-25.

[3]Mukhopadhyay, V., "Blended-Wing-Body (BWB) Fuselage Structural Design for Weight Reduction", AIAA Paper 2005-2349, 46th AIAA/ASME/ASCE/AHS/ASC Structures, Structural Dynamics and Materials Conference, Austin, Texas, April 18-21, 2005.

[4]Velicki, Alex, and Hansen, Dan, "Novel Blended Wing Body Structural Concepts", NRA-03-LaRC-02 Maturation for Advanced Aerodynamic and Structures Technologies for Subsonic Transport Aircraft: Phase I Final Report, July 13, 2004.

[5]Mukhopadhyay, V., Sobieszczanski-Sobieski, J., Kosaka, I., Quinn, G., and Charpentier, C., "Analysis Design and Optimization of Non-cylindrical Fuselage for Blended-Wing-Body (BWB) Vehicle", AIAA Paper 2002-5664, 9th AIAA/ISSMO Symposium on Multidisciplinary Analysis and Optimization, Atlanta, Georgia, September 4-6, 2002.

[6]Vitali, Roberto, Park, Oung, Haftka, Raphael T., Sankar, Bhavani V., and Rose, Cheryl A., "Structural Optimization of a Hat-Stiffened Panel Using Response Surfaces", *Journal of Aircraft*, Vol. 39, No. 1, January-February, 2002, pp. 158-166.

[7]Engels, Heiko, Becker, Wilfried, and Morris, Alan, "Implementation of a Multi-level Optimisation Methodology Within the E-design of a Blended Wing Body", *Aerospace Science and Technology*, Volume 8, 2004, pp. 145-153.

[8]*MSC.NASTRAN 2005 Quick Reference Guide*, Vols. 1 and 2, MSC.Software Corporation, 2004.

[9]*MSC.NASTRAN 2004 Design Sensitivity and Optimization User's Guide*, MSC.Software Corporation, 2003.

[10]*DOT Design Optimization Tools Users Manual*, Version 5.0, Vanderplaats Research and Development, Inc., Colorado Springs, CO, 1999.
[11]Vanderplaats, G. N., "ADS – A Fortran Program for Automated Design Synthesis – Version 1.10, NASA CR 177985, September, 1985.
[12]Holland, J. H., *Adaptation of Natural and Artificial Systems*, The University of Michigan Press, Ann Arbor, MI, 1975.
[13]Goldberg, D. E., *Genetic Algorithms in Search, Optimization, and Machine Learning*, Addison-Wesley Publishing Co. Inc., Reading, MA, 1989.
[14]Reeves, C. R., and Rowe, J. E., Genetic Algorithms – Principles and Perspectives: A Guide to GA Theory, Klewer Academic Publishers, Norwell, MA, 2003.
[15]Chambers, L., editor, *The Practical Handbook of Genetic Algorithms Applications (2nd edition)*, Chapman & Hall/CRC, New York, NY, 2001.
[16]Whitley, L. D., editor, *Foundations of Genetic Algorithms-2*, Morgan Kaufmann Publishers, San Mateo, CA, 1993,

REPORT DOCUMENTATION PAGE

Form Approved
OMB No. 0704-0188

1. REPORT DATE *(DD-MM-YYYY)*	2. REPORT TYPE	3. DATES COVERED *(From - To)*
01- 10 - 2006	Contractor Report	

4. TITLE AND SUBTITLE

Optimization of Blended Wing Body Composite Panels Using Both NASTRAN and Genetic Algorithm

5a. CONTRACT NUMBER

NNL04AA06Z

5b. GRANT NUMBER

5c. PROGRAM ELEMENT NUMBER

6. AUTHOR(S)

Lovejoy, Andrew E.

5d. PROJECT NUMBER

5e. TASK NUMBER

5f. WORK UNIT NUMBER

561581.02.08.07

7. PERFORMING ORGANIZATION NAME(S) AND ADDRESS(ES)

NASA Langley Research Center
Hampton, VA 23681-2199

Analytical Services & Materials, Inc.
107 Research Drive
Hampton, VA 23666-1340

8. PERFORMING ORGANIZATION REPORT NUMBER

9. SPONSORING/MONITORING AGENCY NAME(S) AND ADDRESS(ES)

National Aeronautics and Space Administration
Washington, DC 20546-0001

10. SPONSOR/MONITOR'S ACRONYM(S)

NASA

11. SPONSOR/MONITOR'S REPORT NUMBER(S)

NASA/CR-2006-214515

12. DISTRIBUTION/AVAILABILITY STATEMENT

Unclassified - Unlimited
Subject Category 39
Availability: NASA CASI (301) 621-0390

13. SUPPLEMENTARY NOTES

Langley Technical Monitor: Dawn C. Jegley
An electronic version can be found at http://ntrs.nasa.gov

14. ABSTRACT

The blended wing body (BWB) is a concept that has been investigated for improving the performance of transport aircraft. A trade study was conducted by evaluating four regions from a BWB design characterized by three fuselage bays and a 400,000 lb. gross take-off weight (GTW). This report describes the structural optimization of these regions via computational analysis and compares them to the baseline designs of the same construction. The identified regions were simplified for use in the optimization. The regions were represented by flat panels having appropriate classical boundary conditions and uniform force resultants along the panel edges. Panel-edge tractions and internal pressure values applied during the study were those determined by nonlinear NASTRAN analyses. Only one load case was considered in the optimization analysis for each panel region. Optimization was accomplished using both NASTRAN solution 200 and Genetic Algorithm (GA), with constraints imposed on stress, buckling, and minimum thicknesses. The NASTRAN optimization analyses often resulted in infeasible solutions due to violation of the constraints, whereas the GA enforced satisfaction of the constraints and, therefore, always ensured a feasible solution. However, both optimization methods encountered difficulties when the number of design variables was increased. In general, the optimized panels weighed less than the comparable baseline panels.

15. SUBJECT TERMS

Graphite-epoxy; Buckling; optimization

16. SECURITY CLASSIFICATION OF:			17. LIMITATION OF ABSTRACT	18. NUMBER OF PAGES	19a. NAME OF RESPONSIBLE PERSON
a. REPORT	b. ABSTRACT	c. THIS PAGE			STI Help Desk (email: help@sti.nasa.gov)
					19b. TELEPHONE NUMBER *(Include area code)*
U	U	U	UU	72	(301) 621-0390